One- and Two-Dimensional High-Resolution Solid-State NMR Studies of Zeolite Lattice Structures

C. A. FYFE,* Y. FENG, H. GRONDEY, G. T. KOKOTAILO, and H. GIES

Department of Chemistry, University of British Columbia, Vancouver, British Columbia, Canada V6T 1Z1

Received April 9, 1991 (Revised Manuscript Received August 5, 1991)

Contents

I. Introduction

In recent years, high-resolution solid-state NMR spectroscopy (especially of the ^{29}Si nucleus) has emerged as a powerful complementary method to diffraction techniques for the investigation of zeolite lattice structures. The combination of NMR and XRD is particularly appropriate as the former is most sensitive to local orderings and geometries while the latter is determined by long range orderings and periodicities and when taken together they provide a more complete description of the structure. In this article, we will concentrate particularly on recent work and ongoing developments in the field. A comprehensive review of the literature up to 1986 has been presented by Engelhardt and Michel.[1] In addition, we will restrict our discussion to investigations of the zeolite framework itself.

II. Zeolites

Zeolites are open framework aluminosilicates, widely used in industrial applications as ion exchange resins, molecular sieves, and catalysts and catalyst supports.[2,3] Formally, they can be represented as being derived from silica (SiO_2) by the replacement of SiO_4^{4-} tetrahedra by AlO_4^{5-} tetrahedra and described by the general oxide formula (eq 1), where the part in square brackets represents the lattice.

$$M^{x+}_{y/x}[(AlO_2)_y(SiO_2)_{1-y}]\cdot nH_2O \quad (1)$$

Because of the difference in atomic charge between Al and Si, extra-lattice cations (M^{x+}) must be present to preserve electrical neutrality, a single positive charge needed for each (AlO_2) unit. These cations are not part of the framework and may be easily exchanged. In addition, water of hydration is usually present but also is not part of the lattice structure.

The catalytic activity of zeolites is generated by converting them to an "acid form" by heating the "ammonium form" of the zeolite (where the cations are NH_4^+) to 450 °C. This causes decomposition of the ammonium ions and yields a material where the extra-lattice cations are (at least formally) H^+ (eq 2).

$$NH_4^+ \rightarrow NH_3\uparrow + H^+ \quad (2)$$

This will now act as a very powerful acid catalyst in reactions of hydrocarbons such as isomerizations, alkylations, and hydrogen transfers.

The size- and shape-selective characteristics of zeolites come from their unique framework structures: In general they are formed from open arrangements of AlO_4^{5-} and SiO_4^{4-} tetrahedra linked by sharing oxygen atoms (the Al and Si atoms are often referred to as T (tetrahedral) atoms). Figure 1 shows how the lattice frameworks of several common zeolites can be assembled from a single building unit. The truncated octahedron or sodalite cage subunit (Figure 1A) has faces of 4- and 6-membered rings where the vertices are Si or Al T atoms joined by linking oxygens (not shown). When two of these are joined via 4-membered rings with bridging oxygens, the structure shown in Figure 1B is formed, and linking of two of these units together gives the structure in Figure 1C. This is the basic lattice structure of zeolite-A, commonly used in research laboratories as a "molecular sieve". There is a large central cavity accessible from three orthogonal straight channels. It is this pore and channel structure which gives the lattice its unique size and shape selectivity. Depending on the size of the cations in the cavities, molecules of different sizes will be adsorbed as indicated in the series: Na^+, 4 Å; K^+, 3 Å; and Ca^{2+}, 5 Å. Figure 1, parts D and E show two other zeolites made up from the same basic building block. Figure 1E shows the lattice structure of faujasite (also known as zeolite-X or zeolite-Y depending on the Si/Al ratio if obtained by synthesis) which is widely used as a "cracking" catalyst in petroleum refining. There is again a large central cavity, but in this case the channels are no longer straight. When two units share a 4-membered ring (Figure 1D), the sodalite lattice is formed. In this case the structure is completely space filling (the central "cavity" being identical with the building unit) and this system shows no catalytic or molecular sieving properties at all.

0009-2665/91/0791-1525$09.50/0

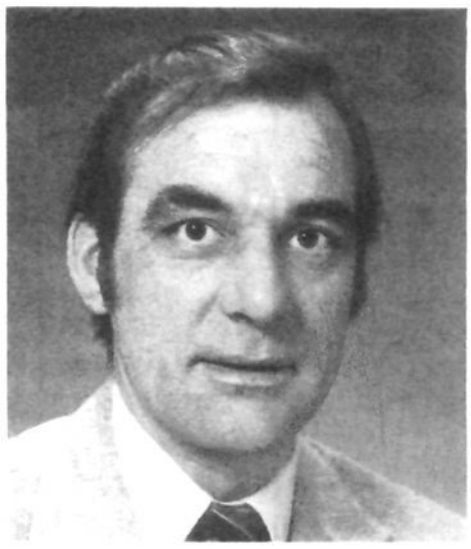

Colin A. Fyfe received his B.Sc. in chemistry from St. Andrews University in 1964 and his Ph.D. from St. Andrews in 1966 under Professor R. Foster. After one year as a Medical Research Council Postdoctoral Fellow at St. Andrews University and two years as a Killam Postdoctoral Fellow at the University of British Columbia he joined the faculty of the University of Guelph obtaining the rank of Professor in 1978. In 1987 he joined the faculty of the University of British Columbia as Professor of Chemistry and Pathology. He has been the recipient of the Merck Sharp and Dohme award for organic chemistry and the Barringer Award for analytical spectroscopy and in 1986 was elected a Fellow of the Royal Society of Canada. His research interests lie in the characterization of synthetic and biological materials by nuclear magnetic resonance spectroscopy, including the use of high-resolution solid-state NMR and NMR microscopic imaging techniques.

Hiltrud Grondey was born and raised in Dinslaken, Germany. She studied physics at the Rheinisch-Westfälische Technische Hochschule Aachen (Germany) and received her diploma in 1985. For her Ph.D. work, she chose a subject from physical chemistry: her thesis, which she defended in 1988 at the Universität-Gesamthochschule Siegen (Germany), was on solid-state NMR spectroscopy of organometallic compounds. From 1989 to 1991, she was with C. A. Fyfe's group as a postdoctoral fellow, and, currently, she is a scientific employee at the Max-Planck-Institut für Kohlenforschung, Mülheim (Germany). Her research interest are new applications and development of NMR techniques.

Yi Feng was born in Shanghai, China. She received her B.Sc. and M.Sc. degrees from Nanjing University, China and carried out her Ph.D. work which involved the application of high-resolution solid-state NMR to the investigation of zeolite structures under the guidance of C. A. Fyfe at the University of British Columbia, Canada. She obtained her Ph.D. degree in 1991 and is currently employed by Arbokem Inc., Vancouver.

Some zeolites have much more complex unit cells and lattice structures than those discussed above, each of which has only a single lattice site. A particularly important example with a very complex unit cell is zeolite ZSM-5, one end being a member of a series of "pentasil" zeolites, the other end being zeolite ZSM-11.[4] The pentasil building unit consists entirely of 5-membered rings and is shown in Figure 2A. Joining these units in columns (Figure 2B) and then joining layers of columns such that the neighboring layers are related by inversion symmetry produces the zeolite ZSM-5 shown in Figure 2D. Joining the columns so that the layers are related by a reflection plane yields the closely related ZSM-11 lattice structure (Figure 2C). Since the two structures differ in only one projection and so many of the repeat distances are similar, their powder X-ray diffraction patterns are quite similar. Zeolite ZSM-5 is a very important catalyst, being extremely size and shape selective toward organic molecules and will be discussed in detail in the present review.

Although zeolites are highly crystalline materials, the structural information which may be obtained by the application of diffraction measurements is severely limited. First, they are microcrystalline, yielding crystals which are too small (usually of the order of microns) for conventional single-crystal diffraction studies and most structure determinations must be attempted from the much more limited powder diffraction data.[5] Second, since Si and Al have relatively high atomic masses and differ by only one mass unit (28 and 27 au, respectively), their X-ray scattering factors are almost identical and it is often not possible to clearly distinguish them. An additional complication is that the Si and Al atoms in zeolites are usually disordered over the T sites and an average structure results. In general, diffraction measurements will at best determine the overall lattice structure, but not define the placement of the individual Si and Al atoms over the T sites within this structure.[5]

III. NMR Characteristics of Nuclei in Zeolite Lattices

All of the atoms making up the zeolite lattice as described by eq 2 have NMR-active isotopes and thus can be investigated by solid-state NMR, that is ^{29}Si (4.6%), ^{27}Al (100%), ^{17}O (0.04%, isotopic enrichment will be necessary here). In addition ^{1}H (100%) may be present in OH groups at defect sites in the framework. We will discuss the kind of information which can be obtained regarding zeolite lattice structures with some emphasis on studies of the ^{29}Si spectra since they give the most direct information on the framework itself.

Further insight can be gained from eq 1 regarding the solid-state NMR experiments: In general, protons in

George Kokotailo was born in Alberta, Canada and received B.Sc. and M.Sc. degrees from the University of Alberta and a Ph.D. from Temple University. He was employed by Canadian Industries Limited and the National Research Council of Canada before joining Mobil Research and Development Corporation in Paulsboro, New Jersey, where he spent 34 years before retiring in 1982. He is an adjunct professor at Drexel University and a visiting professor at the University of British Columbia in Vancouver. He was also an adjunct professor at the University of Guelph. Kokotailo has been the recipient of an Alexander von Humboldt Senior U.S. Scientist Award in 1985 and a second award in 1991. He has over 100 publications and patents. His research interests include the synthesis of zeolites and their characterization by XRD, EM, EPA, NMR, adsorption, diffusion, and catalysis.

Hermann Gies is Professor of mineralogie at the Ruhr-University Bochum, Germany. He received his Ph.D. in inorganic chemistry at the Christian-Albrecht University of Kiel, Germany in 1982. He did postdoctoral research at the University of Aberdeen, Scotland, at the University of Guelph, Canada, at the University of British Columbia, Vancouver, Canada, and at the Christian-Albrechts University, Kiel, Germany, where he received his habilitation in 1988. His current research interests lie in the study of the mechanism of the formation of porous solids, in particular zeolites, and their structural characterization with diffraction and NMR techniques.

the system are present only as water of hydration which is not part of the lattice framework and which will usually be mobile. Thus, the dipolar interactions between the observed nucleus and protons will be small and cross-polarization and cross-polarization techniques for signal enhancement will not be applicable. On the other hand, no high-power proton decoupling is required to remove the dipolar line broadening, and the solid-state NMR experiment on zeolites usually thus reduces to the very simple one of magic-angle spinning only, and this can be easily carried out on a conventional high-resolution NMR spectrometer.[6] Further, the experiments are no more difficult at high magnetic fields and are often best carried out at as high a magnetic field strength as possible. However, there are fundamental differences in the nature of the different nuclei discussed above. ^{29}Si is a spin $^1/_2$ nucleus and MAS yields particularly simple spectra with complete averaging of the chemical shift tensor components. The average "isotropic" values are field independent and correspond to the solution chemical shifts. ^{27}Al and ^{17}O, however, are quadrupolar nuclei with nonintegral spins and their solid-state spectra are more complex as will be discussed in more detail subsequently.

IV. ^{29}Si MAS NMR Studies

As indicated above, ^{29}Si MAS spectra are particularly straightforward and, as we will demonstrate, may be related in a direct manner to the results of X-ray diffraction studies. In this section, we describe the development of these techniques.

A. Investigations of Low Si/Al Ratio Zeolites

Since the initial work of Lippmaa and Engelhardt,[7] there have been a large number of studies of the ^{29}Si MAS NMR spectra of low Si/Al ratio zeolites. The general features of these spectra are now well understood and the results from these early studies have been reviewed.[1] In general, the ^{29}Si MAS NMR spectra of simple zeolites show a maximum of five reasonably well resolved peaks as illustrated in Figure 3 for the zeolite analcite. It was demonstrated by Lippmaa and Engelhardt[7] that these five peaks corresponded to the five possible distributions of Si and Al around a silicon nucleus at the center of an SiO_4 tetrahedron, i.e. Si[4Al], Si[3Al,1Si], Si[2Al,2Si], Si[Al,3Si], and Si[4Si] as indicated in the figure. Further, the chemical shift ranges over which the resonances occur are reasonably characteristic of the composition of the first coordination sphere as shown in Figure 4, and the spectra may thus be used to probe the local Si/Al distributions in simple zeolite lattices. A particularly important application is that the Si/Al ratio of the lattice can be calculated directly from the ^{29}Si spectra. This has been investigated in detail for the zeolite faujasite (also known as zeolite-X or -Y) which can be obtained by direct synthesis with the same basic structure but over a wide range of compositions (Si/Al = 1–3). Typical results are shown in Figure 5 together with the Si/Al ratios calculated from the ^{29}Si spectra.[9] As the Si/Al ratio increases, there is a corresponding increase in the relative intensities of the high-field peaks as would be expected from the peak assignments above. Assuming "Loewenstein's rule" (10) which postulates that Al–O–Al linkages do not occur in these systems, it can be shown that the Si/Al ratio may be calculated from the peak areas of the five peaks in the ^{29}Si spectrum according to eq 3.

$$\frac{\mathrm{Si}}{\mathrm{Al}} = \frac{\sum_{n=0}^{4} I_{\mathrm{Si}(n\mathrm{Al})}}{\sum_{n=0}^{4} 0.25n[I_{\mathrm{Si}(n\mathrm{Al})}]} \qquad (3)$$

Compared to traditional bulk chemical analysis, this method has the advantage that it detects the Al atoms indirectly from their affect on the Si atoms *in the framework* and thus only detects framework Al atoms and the *Si/Al ratio for the framework*, whereas the

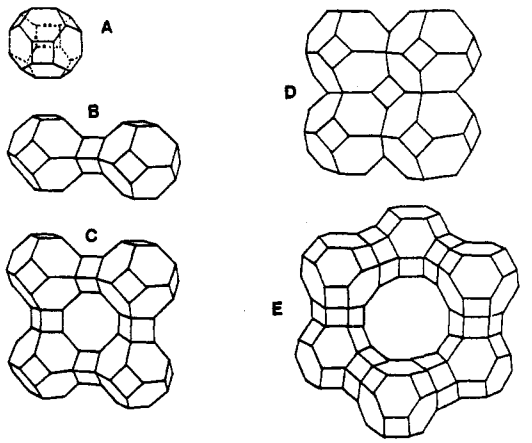

Figure 1. Lattice structures of typical zeolites formed from the sodalite cage building block (see text).

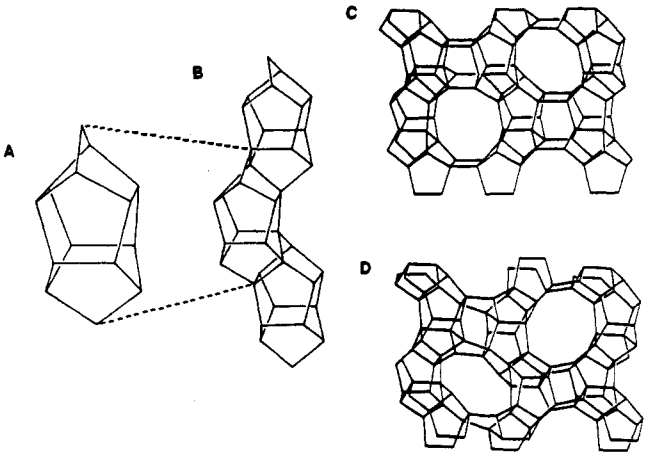

Figure 2. Schematic representations of (A) the pentasil unit, (B) a chain formed by interlocking pentasil units, and the structures of (C) zeolite ZSM-11 and (D) zeolite ZSM-5.

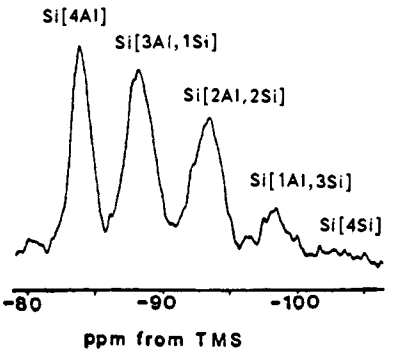

Figure 3. ^{29}Si MAS NMR spectrum of the zeolite analcite (79.6 MHz).

ratio from chemical analysis will include both framework Al and any Al occluded in the cavities or present as impurities and not an integral part of the system. The two analyses will thus be complementary.

There is a natural tendency to attempt the deduction of specific Si, Al distributions within the lattice from the ^{29}Si NMR data, but the NMR results reflect the local environments of the Si atoms averaged throughout the lattice (and also all the crystals in the sample) and do not necessarily imply any simple long-range ordering. However, they have been successfully used by Melchior[11] to investigate differences in the formation mechanisms of zeolites-A and -Y which show quite different distributions of the local environments for

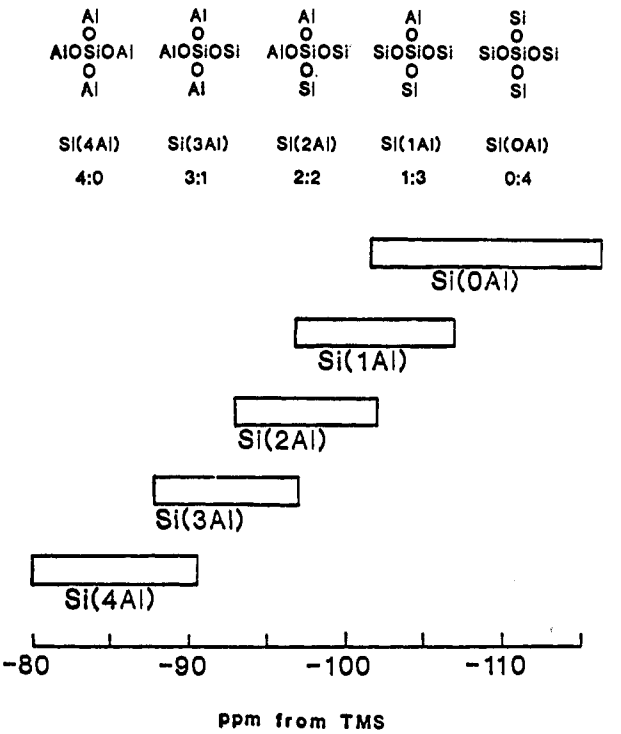

Figure 4. Characteristic chemical shift ranges of the five different local silicon environments (adapted from ref 8).

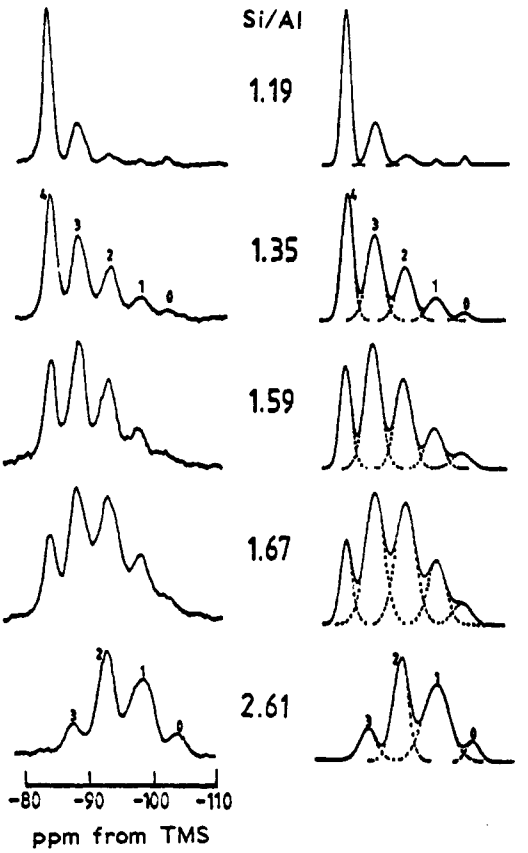

Figure 5. Observed and calculated ^{29}Si MAS NMR spectra of faujasite zeolites with the Si/Al ratios indicated (from ref 9).

identical Si/Al ratios.

As indicated above, the simple MAS experiment yields spectra which are quantitatively reliable as long as care is taken to allow for the nuclear relaxation process. In general, cross-polarization yields spectra of much poorer S/N, but has an important application.

The detection of $Si(OR)_3OH$ groupings which occur as defects (and which are of interest because of potential involvement in catalysis) can be facilitated by the use of cross-polarization techniques which discriminate greatly in favor of silicon atoms close to the OH groups in the lattice.[12] This is illustrated in Figure 6 which shows a marked increase in the relative intensity of the signals at ~−104 ppm. However, care must be taken in the interpretation of such CP/MAS spectra because they are nonquantitative in nature and indicate only that some Si(OH) units are present, not that they are the only units contributing to the signal at this shift in the MAS spectrum. The corresponding spectra from 90° pulses indicate that the *proportion* of these functionalities is small, but the CP technique is extremely useful in indicating their presence.

B. ^{29}Si MAS NMR Studies of Highly Siliceous Zeolites

More recently, considerable information has been obtained from the ^{29}Si MAS NMR spectra of highly siliceous zeolites, where the Al content is so low that it does not affect the ^{29}Si spectrum.[13] Materials of this type may be synthesized directly and can also be obtained by removal of Al from low Si/Al systems by chemical treatments. For example, $SiCl_4$ may be used in some systems to replace the lattice aluminum atoms or they may be removed by treatment with water vapor at elevated temperatures. Where the Si/Al ratio is already high from the synthesis, these procedures may be used to remove any residual aluminum.

The hydrothermal dealumination procedure described by eq 4 is particularly versatile and can be used to produce a large variety of highly siliceous zeolites.

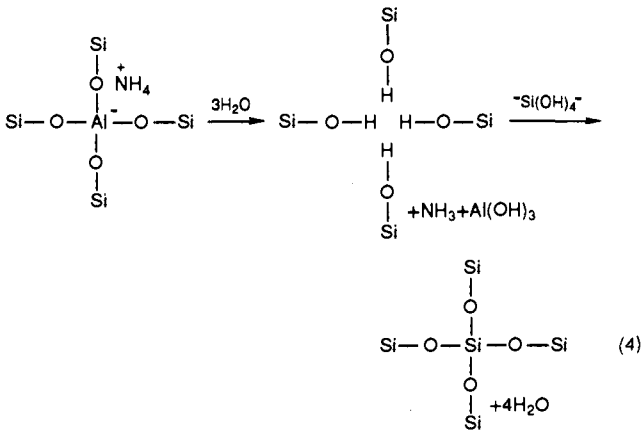

(4)

Even zeolite-A, which is known to be both thermally and chemically unstable, may be produced in completely siliceous form by hydrothermal treatment of the high silica analogue ZK-4.[14] Figure 7 shows the ^{29}Si MAS NMR spectra of the highly siliceous forms of some typical zeolites together with those of the corresponding low Si/Al ratio forms.[15,16] In all highly siliceous materials, the resonances observed are due to only Si[4Si] groupings and are extremely narrow. Because of their excellent resolution, these spectra can be exploited in a number of ways to obtain subtle information regarding zeolite structures, not easily obtainable by other techniques.

The line widths of the ^{29}Si resonances for low Si/Al ratio materials are of the order of 5–8 ppm which is

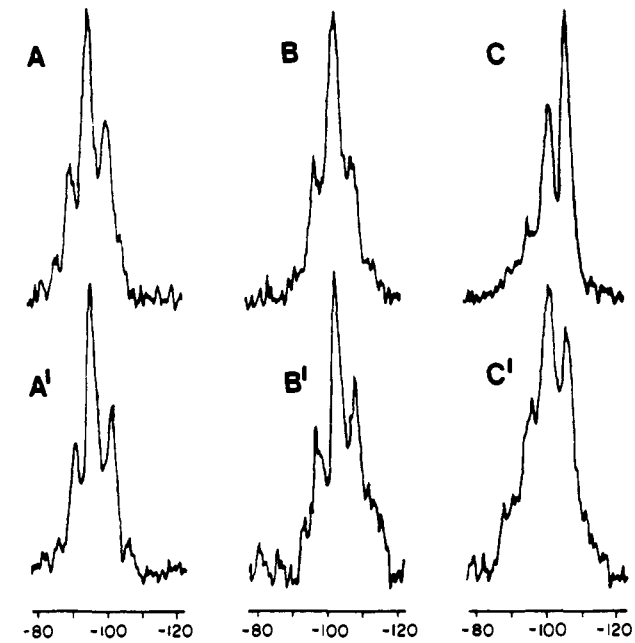

Figure 6. ^{27}Si MAS NMR spectra of dealuminated zeolite-Y without (upper spectra) and with cross-polarization (lower spectra). A and B are the spectra from the starting NaY material. The other samples have been dealuminated to varying degrees (from ref 12).

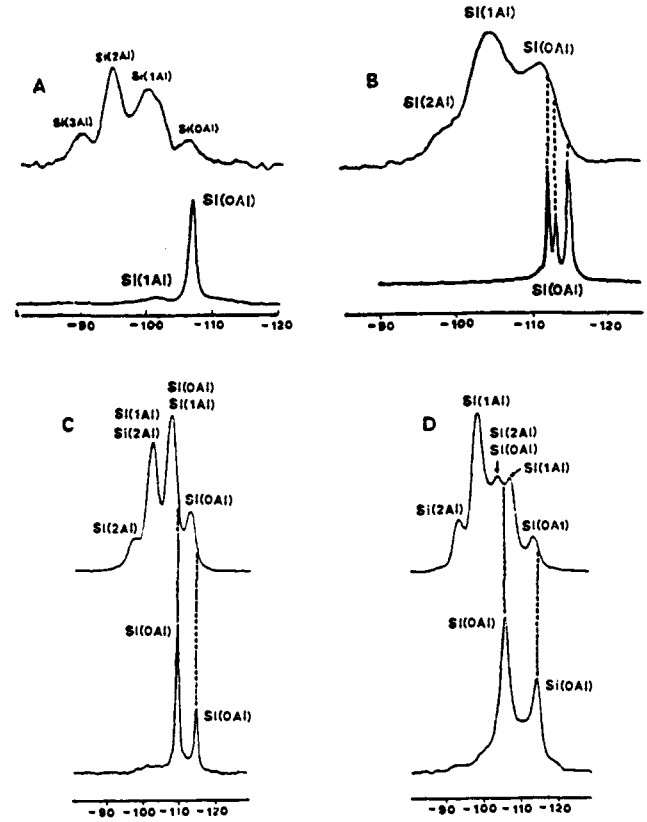

Figure 7. ^{29}Si MAS NMR spectra of the highly siliceous and corresponding low Si/Al ratio forms of (A) zeolite-Y, (B) mordenite, (C) offretite, and (D) zeolite-Ω (adapted from refs 15 and 16).

surprisingly large considering their highly crystalline nature. (For comparison, line widths in the ^{13}C spectra of highly crystalline organic solids are of the order of 1 ppm or less.) From Figure 7, it can be seen that the removal of Al from the zeolite framework reduces the line widths to ~1 ppm, indicating that the Al atoms

in these systems are responsible for the line broadening. It is possible that this is due to residual dipolar interactions to the quadrupolar ^{27}Al nuclei which are not completely removed by MAS, but this is unlikely at the high fields used. Careful inspection of the spectra in Figure 7 reveals that not only do the resonances narrow, but they also shift to the very high field extreme of the Si[4Si] peak in the corresponding low Si/Al ratio materials.[16] This upfield shift indicates that the residual broadening in the ^{29}Si MAS NMR spectra of low Si/Al ratio zeolites is due to a chemical shift distribution arising from a range of environments due to different possible distributions of Si and Al in second and further nearest neighbors. Thus, the broadening of the spectra reflects *disordering* in the lattice: It is not how much Al is present, but rather how it is distributed. This is confirmed by the ^{29}Si MAS NMR spectra of the gem-quality minerals albite and natrolite and of zeolite-A, all of which are perfectly ordered and which have narrow ^{29}Si resonances of the order of 1 ppm even though the different silicon nuclei in these systems all have one or more aluminum atoms as first nearest neighbors.

C. Crystallographically Inequivalent Sites from ^{29}Si Spectra

The ^{29}Si spectra of highly siliceous zeolites can be directly related to their framework structures. Thus, the numbers and relative intensities of the sharp resonances which are observed reflect directly the numbers and occupancies of the crystallographically inequivalent T sites in the asymmetric unit of the unit cell.

In the cases of both faujasite and zeolite-A, there is a single unique lattice site and the completely siliceous analogues both show single sharp signals. The mordenite structure has $16T_1$ $16T_2$, $8T_3$, and $8T_4$ sites. There are three resonance lines in the NMR spectrum with relative intensities of 2:1:3 which means that two of the resonances are accidentally degenerate. The spectrum of zeolite-Ω which has the mazzite structure with $24T_1$ and $12T_2$ sites shows only two resonances with relative intensities 2:1 which may thus be unambiguously assigned. Similarly, the two resonances in the offretite spectrum may be assigned to the $12T_1$ and $6T_2$ sites in the unit cell. For other highly siliceous zeolites, similar assignments can be made, giving a direct correlation between the NMR and XRD experiments.

However, the spectra in Figure 7 also indicate that the interpretation of the ^{29}Si MAS NMR spectra of zeolites with more than one independent T site in the unit cell may be much more complex than we have indicated up to this point as the effects of site inequivalence as well as that of Al in the first coordination sphere must now be considered. (The systems originally investigated in the deduction of Figure 4 were somewhat atypical in this regard as they had lattices which contained only one unique T site.) In the case of mordenite, the shift dispersion is limited and acts mainly as an additional line-broadening mechanism in the spectrum of the low Si/Al ratio material. However, in the case of offretite, the shift difference due to T-site inequivalence (5.3 ppm) is almost exactly the same as the effect of Al in the first coordination sphere as discussed earlier and there is exact overlap of the different peaks giving the assignments indicated in the figure.

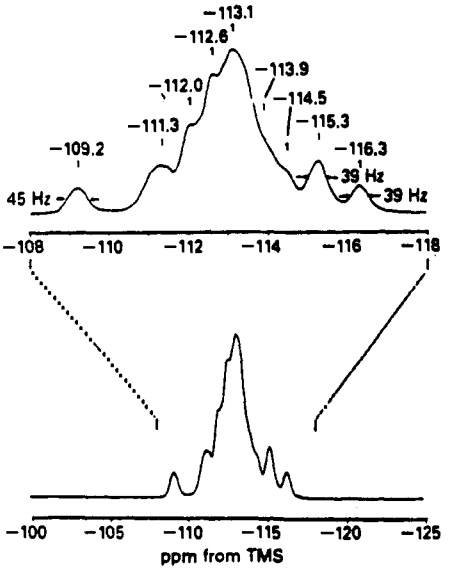

Figure 8. ^{29}Si MAS NMR spectrum (79.6 MHz) of highly siliceous zeolite ZSM-5 (from ref 19).

Particularly important is that the simple formula given in eq 3 for calculating the Si/Al ratio is invalid since it relates only to systems with single T sites and more complex treatments must be undertaken. However, the offretite system is underdetermined and the distributions of the silicon atoms over the two sites for each of the coordinations cannot be deduced from the ^{29}Si spectrum alone without other assumptions regarding the randomness of the distribution. From the results from the case of zeolite-Ω such assumptions should not be made. In the ^{29}Si spectrum of zeolite-Ω, the shift difference between the T sites is 8.5 ppm which is larger than the first coordination sphere influence of Al.[17] In this case, an unambiguous assignment of all of the silicon atoms over the two T sites for each of the local environments may be made by using the Si/Al ratio found by chemical analysis as a correct estimate for the lattice, but without any assumptions at all regarding the nature of the Al distribution. Most importantly, the distribution of Al over the two T sites is predicted to be 1.7:1 which can be directly confirmed from the ^{27}Al MAS NMR spectrum obtained at 14.1 T (600 MHz for protons) showing that the Si/Al distribution is nonrandom in nature.

Good examples of the utility of the ^{29}Si spectra of highly siliceous systems, their direct relationship to diffraction structures and sensitivity to local effects come from investigations of the ZSM-5 system described earlier. The ZSM-5 and ZSM-11 structures are very similar and this is reflected in their XRD patterns. However, because the ^{29}Si chemical shifts are determined by local geometric effects, the ^{29}Si MAS NMR spectra of highly siliceous samples of these two materials are quite different and provide very sensitive 'fingerprints' of the two unit cells.[18] In the case of ZSM-5, the relative intensities of the resolved low- and high-field resonances to the total spectral intensity reveal that there is a total of 24 independent T atoms in the unit cell of the (calcined) ZSM-5 lattice (Figure 8[19]) defining the symmetry of this form as being monoclinic.

The ^{29}Si MAS NMR spectrum of dealuminated ZSM-5 is changed by the sorption of small amounts of *p*-xylene and other organic molecules (Figure 9) with

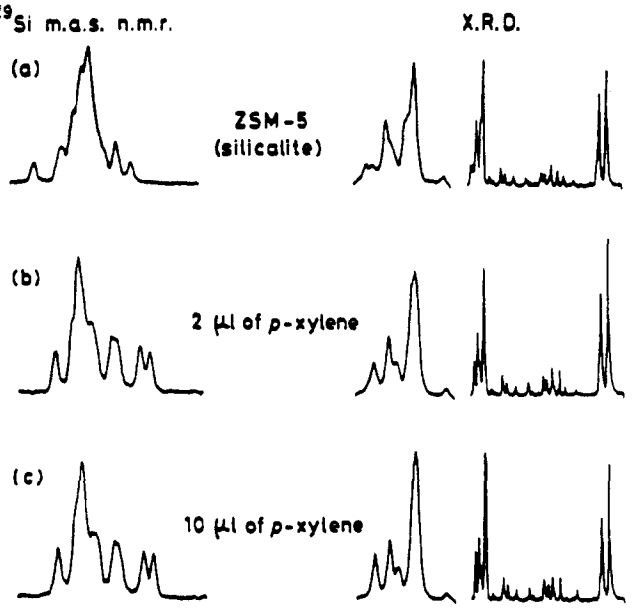

Figure 9. ^{29}Si MAS NMR spectra of highly siliceous ZSM-5 and this material treated with *p*-xylene together with the corresponding XRD patterns (adapted from ref 20).

small related changes in the corresponding XRD patterns. Different organic molecules give characteristic limiting spectra and the changes are completely reversible. Molecules which are very small or too large to be accommodated in the lattice (e.g. *o*-xylene) cause no major changes in the spectra.[20,21] The XRD patterns show small changes indicating transformation from monoclinic to orthorhombic symmetry with the loss of the characteristic "doublet" at $2\theta = 24.4°$. Changes observed in the XRD lines at $2\theta = 23.3°$ and $2\theta = 23.8°$ clearly indicate, in agreement with the NMR data, that structural changes in the lattice are occurring which are characteristic of the sorbate, while the sample crystallinity is maintained intact.

The framework of highly siliceous ZSM-5 is also affected by temperature.[22,23] ^{29}Si MAS NMR spectra recorded between 300 and 377 K show gradual changes in the spectrum with movement of some resonances which may be due to a general expansion of the lattice and then a discrete change between 355 K and 370 K. The limiting high-temperature ^{29}Si spectrum indicates that the spectral changes are due to a phase transition from monoclinic (24 T sites) to orthorhombic (12 T sites) symmetry. These two effects will be subsequently discussed in more detail.

D. Ultra-High-Resolution ^{29}Si Spectra of Highly Siliceous Zeolites

From the foregoing discussion, it can be seen that the ^{29}Si spectra of highly siliceous systems yield considerable information regarding the details of the structures and that they can be directly related to the diffraction data in a very complementary manner. The limiting factor at this point is the resolution of the spectra. This can be improved by very careful shimming of the magnetic field over the whole sample volume and precise setting of the magic angle and stable sample spinning. However, the line widths will also be affected by the perfection of the local ordering within the structure. Thus, further improvements can be gained by the synthesis of extremely highly crystalline samples. The

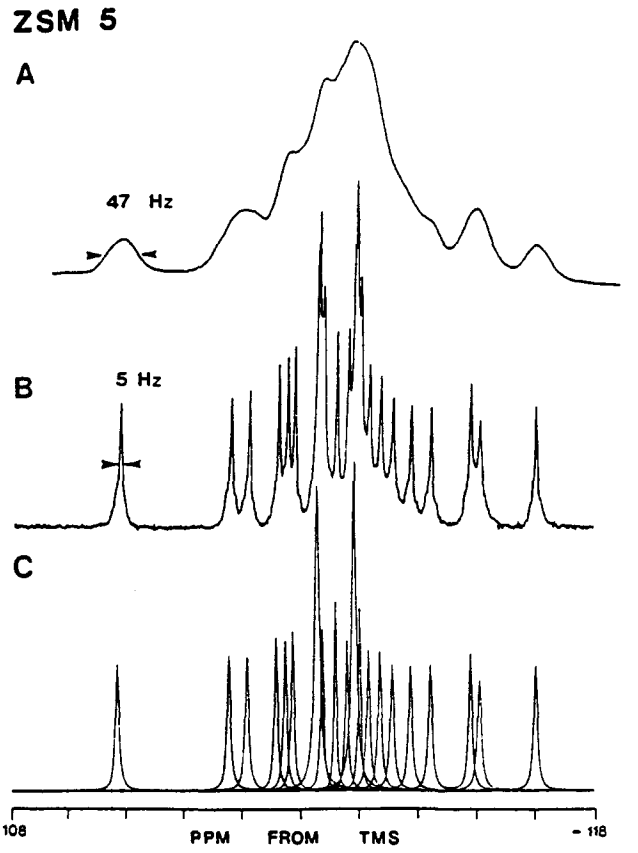

Figure 10. ^{29}Si MAS NMR spectra of very highly crystalline ZSM-5 showing the effect of optimization of all experimental variables (reprinted from ref 25; copyright 1987 American Chemical Society).

effect of careful optimization of all of these different factors is shown in Figure 10 for zeolite ZSM-5. The quality of the spectrum is now such that 21 or 22 of the 24 postulated signals can be clearly observed, depending on the exact temperature of the measurement. The improved resolution of the spectrum now makes it possible to investigate the effects of temperature and sorbed organics in considerable detail.

For comparison with the previous data, the spectra of ZSM-5 in the presence of sorbed organics and at 120 °C are shown in Figure 11. It is clear that the organics induce changes in the lattice which are quite characteristic of the organic sorbate present.[25] *p*-Xylene induces a change to a form with 12 inequivalent T sites (Figure 11) whereas pyridine and acetyl acetone induce changes to new forms which still have 24 T sites. Raising the temperature also causes a change to a 12 T site structure (Figure 11), but the mechanism of the change is different.

The effect of *p*-xylene adsorption at ambient temperature on the ^{29}Si MAS NMR spectrum of highly siliceous ZSM-5 as a function of concentration is shown in Figure 12. At low loading (<0.4 molecules/unit cell) the effect on the spectrum is minimal, with small shifts in individual peaks. At 1.6 molecules/unit cell the spectrum is completely different and now shows only 12 resonances indicating a complete transformation to the orthorhombic form in agreement with XRD data. The NMR spectra indicate that different proportions of both orthorhombic (12 T atoms) and monoclinic (24 T atoms) phases are present in the intermediate loadings. The change in relative intensity of some of the

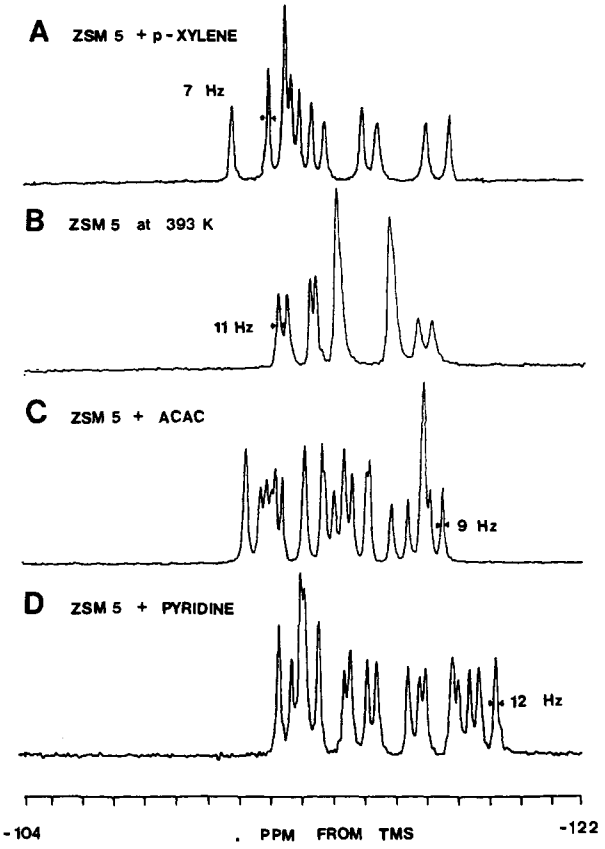

Figure 11. ^{29}Si MAS NMR spectra of ZSM-5: (A) 393 K; (B) 298 K plus *p*-xylene; (C) 298 K plus pyridine; (D) 298 K plus acetylacetone (reprinted from ref 25; copyright 1988 American Chemical Society).

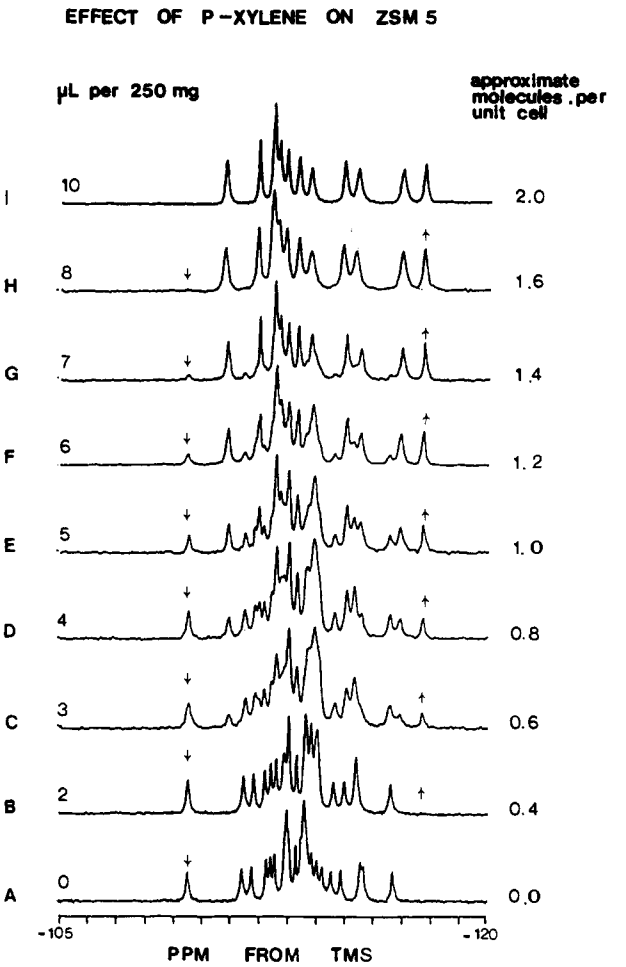

Figure 12. Effect of *p*-xylene on ZSM-5 at ambient temperature (reprinted from ref 25; copyright 1988 American Chemical Society).

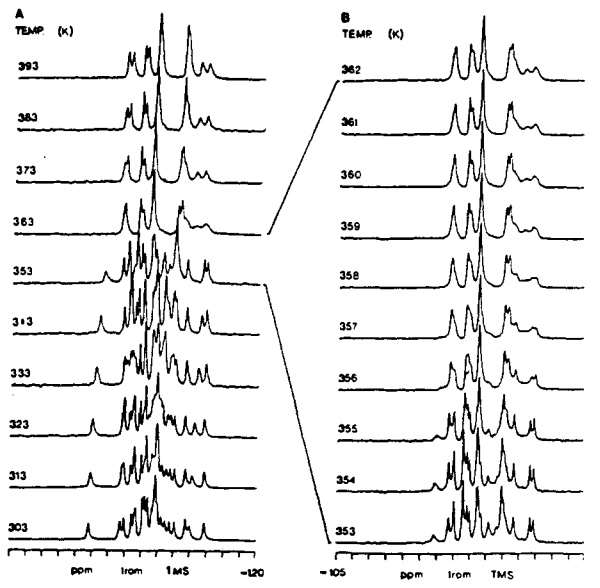

Figure 13. Effect of temperature on ZSM-5 (reprinted from ref 25; copyright 1988 American Chemical Society).

better-resolved resonances indicates the midpoint of the transition at 1 molecule/unit cell with a complete transition at less than 2 molecules/unit cell.

As in the case of sorbed species, the effect of raising the temperature is to induce a phase transformation from monoclinic to orthorhombic. Detailed spectra at 10-degree intervals shown in Figure 13 show gradual shifts of individual resonances up to 353 K with a rapid change between 353 and 363 K. This is confirmed by synchrotron X-ray diffraction analysis of the phase transformation as a function of temperature, which also shows that above the transition temperature only a single phase (the orthorhombic) persists. The combined effect of temperature and organic sorbate is to lower the phase transition temperature and to increase its width. In the phase transition temperature range, both phases now coexist with *all* the material being crystalline. Above the transition temperature, there are only minor changes reflecting lattice expansion due to temperature within the orthorhombic (12 T atom) phase.

The NMR data may now be used in a quite unique way to construct a three-dimensional phase diagram, that is, a plot of the percentage of orthorhombic form present as a function of both sorbate concentration and temperature as shown in Figure 14.[25] This can now be used to determine the limiting conditions under which the different structures exist in phase-pure forms and synchrotron X-ray data can be collected on exactly these characterized structures.

Although the structural changes shown by ZSM-5 with temperature and sorbed organics are not universal for all zeolites, they are not restricted to this system alone. Zeolite ZSM-11, the other end member of the pentasil family of zeolites, crystallizes in the tetragonal system with space group $I\bar{4}m2$.[26] It is very difficult to synthesize pure ZSM-11 without intergrowths or stacking faults, so that for *hkl* reflections, $h + k + l = 2n$ and the doublets merge into singlets. ^{29}Si MAS

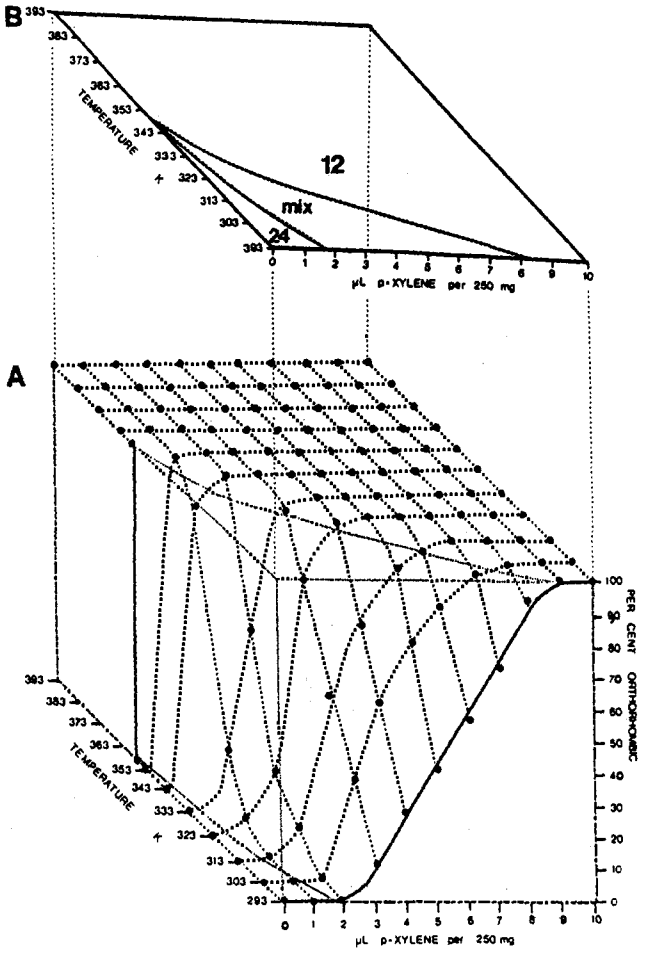

Figure 14. Effects of *p*-xylene and temperature on the crystal symmetry of ZSM-5 (reprinted from ref 25; copyright 1988 American Chemical Society).

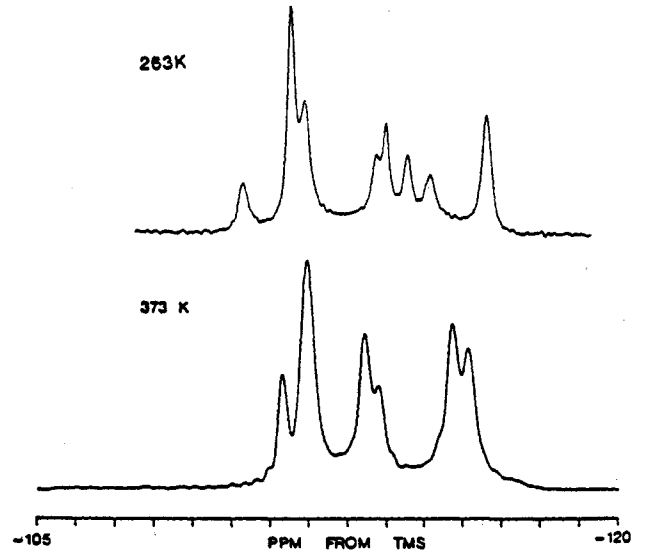

Figure 15. ^{29}Si MAS NMR spectra of zeolite ZSM-11 at 263 and 373 K as indicated (adapted from ref 27b; copyright 1989 American Chemical Society).

NMR spectra of a highly dealuminated and phase-pure ZSM-11 sample have been obtained as a function of temperature.[27] As in the case of ZSM-5 where elevated temperatures promote a transition to a phase of higher symmetry, it was found that at a temperature of 373 K (Figure 15) the spectrum is resolved into six sharp Lorentzian peaks with relative intensities 1:(2 + 2):2:1:2:2 which is consistent with the proposed tetragonal structure, with space group $I\bar{4}m2$, where the six resonances observed are due to the 7 independent Si atoms in the ideal framework structure [16-(T_2,T_3,T_4,T_5,T_7)8(T_1,T_6)]. At room-temperature, the symmetry is lower and the limiting structure is reached only at −20 °C Figure 15). X-ray data can be obtained on the limiting forms of the lattice as before. Rietveld refinement of the data from the high-temperature form yields exactly the previously proposed structure, but the room temperature data do not refine smoothly. As in the case of ZSM-5, the effect of sorbed molecules on the ^{29}Si MAS NMR spectra of ZSM-11 is thought to be a modification of the framework structure which alters the local T-atom environment. This is confirmed by the small but significant changes observed in the XRD patterns which are reversible on desorption.

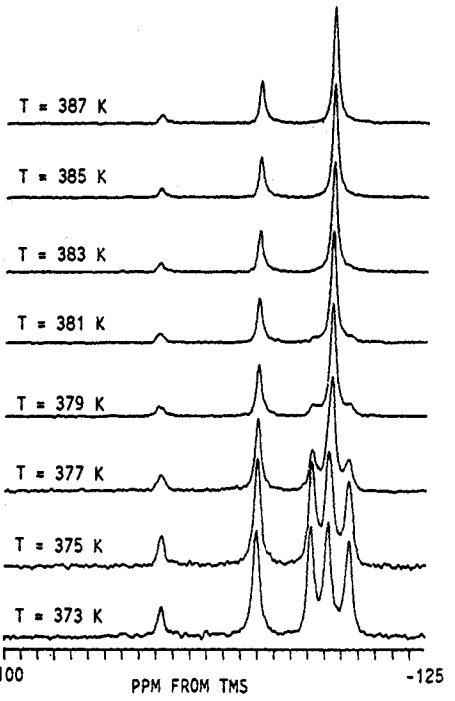

Figure 16. ^{29}Si MAS NMR spectra of zeolite ZSM-39 at the temperatures indicated (reprinted from ref 31; copyright 1987 American Chemical Society).

A particularly clear structural change is observed in the case of zeolite ZSM-39 which is the silicate analogue of the 17Å cubic gas hydrate.[28] Its structure was proposed by Schlenker et al.[29] and refined from single-crystal data in the space group $Fd3$ by Gies et al.[30] However, X-ray powder patterns of the room temperature form show a few very weak extra reflections indicating a space group symmetry lower than face-centered cubic as noted by the authors.[29] There are three independent atoms in the ideal face-centered cubic structure of ZSM-39: 8(T_1), 32(T_2), and 96(T_3). In the ^{29}Si MAS NMR spectrum, the T_3 resonance is split into 3 resonances of equal intensity making the relative spectral intensities 1:4:4:4:4. This splitting is probably due to the removal of the 3-fold symmetry axis. The ^{29}Si NMR spectra obtained over the temperature range 373–383 K are shown in Figure 16. As the temperature is raised, all the resonances remain sharp but there is a clear change over a 10-degree temperature range to a new spectrum which shows three resonances with relative intensities 1:4:12 clearly indicating face-centered

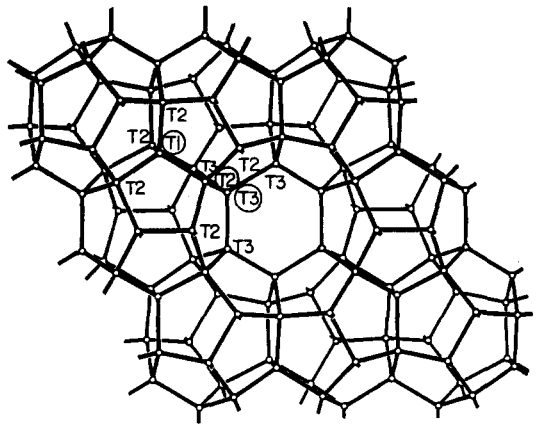

Figure 17. Schematic representation of the zeolite ZSM-39 lattice framework. The three crystallographically inequivalent tetrahedral lattice sites are indicated by T_1, T_2, and T_3 (inside circles), and in each case the identities of the four nearest neighbors are shown.

cubic symmetry, at least on a local basis on the NMR time scale. The changes are completely reversible and also apply to samples with less well resolved spectra.[31]

E. Three-Dimensional Si–O–Si Lattice Connectivities from Two-Dimensional ^{29}Si MAS NMR

As indicated in the previous sections, ^{29}Si MAS NMR can provide a wealth of structural information on zeolites, limited in the case of highly siliceous samples only by the spectral resolution. In solution NMR studies, the application of 2D techniques has provided a wealth of information on the two-dimensional connectivities between atoms within molecular structures.[32] For example, the HSC (heteronuclear shift correlation) sequence establishes heteronuclear connections such as ^{13}C/^{1}H, ^{29}Si/^{1}H, etc., the COSY sequence defines homonuclear correlations, such as ^{1}H/^{1}H, ^{31}P/^{31}P, ^{29}Si/^{29}Si, etc., the INADEQUATE sequence ^{13}C/^{13}C in natural abundance, while longer range connectivities, such as ^{1}H/^{1}H/^{13}C, can be probed by the RCT (relayed coherence transfer) sequence.

A number of 2D NMR experiments have been introduced in high-resolution solid-state NMR studies, for example, to investigate chemical exchange processes,[33] to retrieve chemical shift anisotropies[34] and dipolar couplings,[35] and to probe spin-diffusion processes.[36] Opella has proposed an internuclear distance determined spin-diffusion mechanism in molecular crystals,[37] and Benn and co-workers have demonstrated ^{13}C/^{13}C connectivities using the INADEQUATE sequence for the plastic crystal camphor and have used the COSY sequence for ^{29}Si/^{29}Si connectivities in the reference molecule Q_8M_8.[38]

At least in principle, 2D NMR techniques can be used to establish connectivities in the solid state, and for crystalline three-dimensional framework structures (in contrast to the case of molecular crystals), these connectivities could be used to define the three-dimensional lattice itself. In the present section, we examine the potential of 2D ^{29}Si MAS NMR measurements involving scalar coupling interactions to establish three-dimensional Si–O–Si lattice connectivities in zeolite framework structures. The first system investigated by these techniques was zeolite ZSM-39.[39,40] In order to facilitate the measurements, a small quantity of this material was synthesized which was enriched to ~85% in ^{29}Si. From the known structure shown in Figure 17[29] the connectivities can be worked out. Neglecting the deviation from cubic symmetry which lifts the degeneracy of the T_3 site, the connectivities between the T sites are the following: T_1 is connected to 4 T_2 sites; T_2 is connected to 1 T_1 and 3 T_3 sites; T_3 is connected to 1 T_2 and 3 T_3 sites. Within the unit cell there are, therefore, omitting self-connectivities, 32 T_1T_2 connectivities, 96 T_2T_3 connectivities, and no direct connectivities between T_1 and T_3. In this particular case it is possible to cross-polarize from protons in the template molecule to the silicons in the framework, greatly increasing the efficiency of the experiment as it now depends on only the ^{1}H T_1 which is 3s compared to the ^{29}Si T_1 of 650s. The line widths of the ^{29}Si resonances at 373 K are all 40 Hz or less and indicate a high degree of crystallinity. Determination of connectivities based on scalar couplings is less ambiguous as the couplings are through connecting bonds. Thus, a COSY experiment was attempted by using the conventional sequence from solution NMR studies except that the initial 90° pulse was replaced by a cross-polarization sequence as shown in Figure 18. The fixed delay (FD) in the sequence was optimized experimentally to maximize the cross-peaks. Figure 19 shows the results of a 2D COSY experiment at 373 K using the parameters given in the figure caption. As indicated in the figure, T_1T_2 and T_2T_3 cross-peaks are clearly observed as would be expected from the known structure. The structure of the T_2T_3 cross-peak is real and is due to the partial resolution of the T_3 resonance as shown in Figure 17. Identical connectivities were found by two-dimensional spin-diffusion experiments based on dipolar interactions, but data based on scalar couplings are preferred because they operate through the Si–O–Si bonding network.

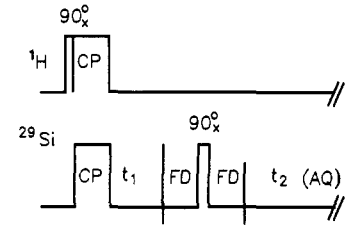

Figure 18. Schematic representation of the modified COSY experiment used in the investigation of ZSM-39.

In a further study using ^{29}Si-enriched material, the three-dimensional bonding in zeolite DD3R was successfully investigated by both COSY and INADEQUATE experiments.[41] At high temperature, the experiments confirmed the symmetry of the structure as that proposed from a single-crystal diffraction experiment,[42] but the room temperature structure was found to be of lower symmetry. There are seven T sites in the high symmetry form and the agreement between the connectivities found with those predicted from the structure rule out the possibility of the agreements in the case of ZSM-39 being fortuitous.

However, the use of ^{29}Si isotopic enrichment in the above investigations is a severe limitation in the application of these techniques, and investigations were attempted by using natural abundance materials[43,44] on the typical zeolite systems ZSM-12 and ZSM-22.

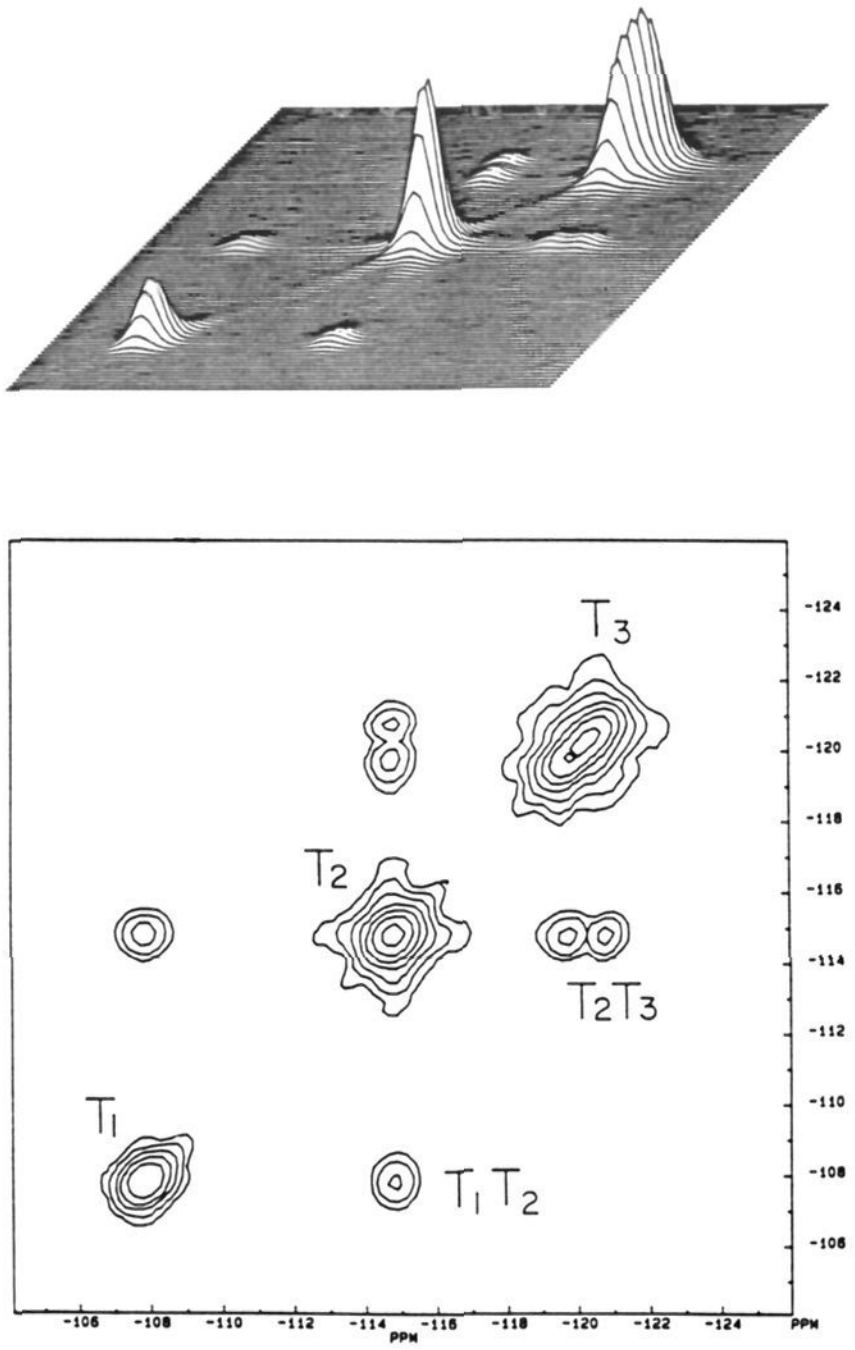

Figure 19. Contour and stacked plots of a 2D COSY experiment on ZSM-39 at 373 K using the pulse sequence of Figure 18 with 128 experiments, 64 scans in each experiment, 5 kHz sweep width, 256 data points for acquisition, and a fixed delay of 5 ms. Sine-bell apodization was used, and the data are presented without symmetrization or smoothing. The total experimental time was approximately 23 h (reprinted from ref 40; copyright 1989 American Chemical Society).

TABLE I. T Atom Sites, Their Occupancies, and Connectivities for the Asymmetric Unit in Zeolite ZSM-12

T site	occupancy	connectivities
T_1	1	$2T_2$:$2T_3$
T_1	1	$2T_1$:$2T_4$
T_3	1	$2T_1$:$1T_5$:$1T_7$
T_4	1	$2T_2$:$1T_5$:$1T_6$
T_5	1	$1T_3$:$1T_4$:$2T_6$
T_6	1	$1T_4$:$2T_5$:$1T_7$
T_7	1	$1T_3$:$1T_6$:$2T_7$

Figure 20 shows one projection of the lattice structure of zeolite ZSM-12. The structure is approximately that originally reported[45] although a recent refinement of synchrotron powder X-ray data by Gies and co-workers[46] establishes the unit cell symmetry as C_2/C with a doubling of the c cell dimension to 24.3275 Å. The number of crystallographically inequivalent silicons in the unit cell is unchanged, there being 7 T sites with equal occupancies as indicated in the figure. This is reflected in the ^{29}Si MAS NMR spectrum which shows seven clearly separated resonances of equal intensities. Table I lists the predicted connectivities from the structure.

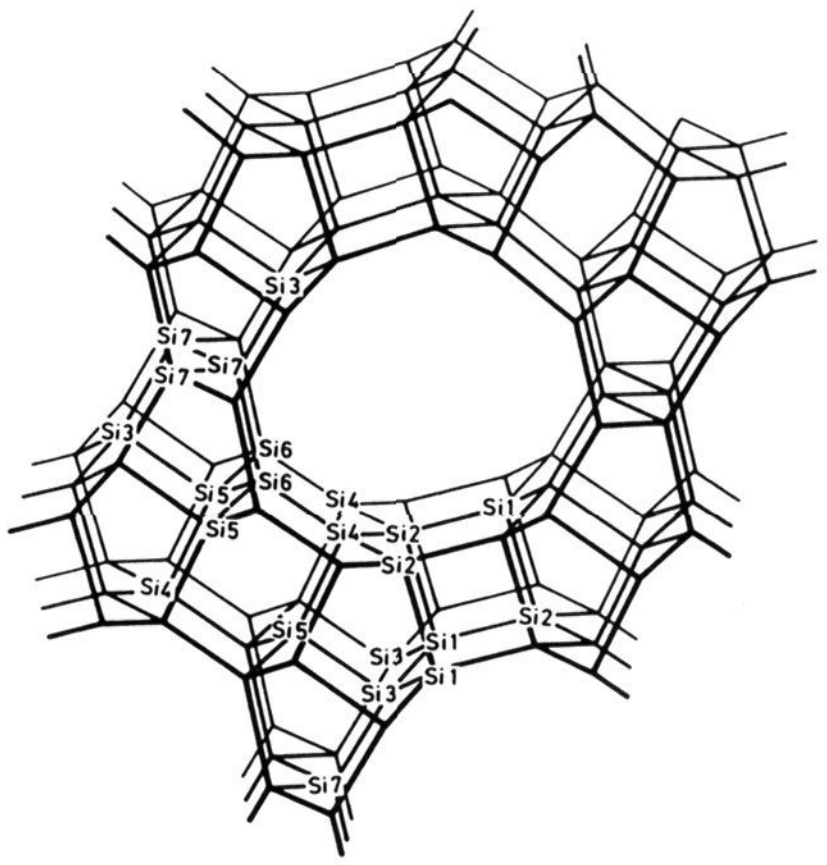

Figure 20. Schematic representation of the zeolite ZSM-12 lattice framework. The seven crystallographically inequivalent tetrahedral lattice sites are indicated by T_1, T_2, ..., T_7 (reprinted from ref 44; copyright 1990 American Chemical Society).

From previous experiments with highly isotopically enriched materials it was seen that the T_2* value (as reflected in the line width) was the determining factor in these experiments, limiting the maximum time which could be used for the frequency encoding and evolution steps quite independently of the magnitude of the J couplings anticipated. By careful shimming and setting of the magic angle, line widths of ca. 8–10 Hz were obtained for the ZSM-12 sample (Figure 20). A 2D COSY experiment[47] consisting of 64 individual experiments with a time increment of 834 μs was used together with a fixed delay of 5 ms for a total maximum t_1 period of 63 ms in the $[(90°)_{\phi_1}$–t_1–$(45°)_{\phi_1}$–acquire] sequence. The results are shown in Figure 21 with the data in the t_2 domain truncated to 256 data points before zero filling. Clear connectivities are observed in the unsymmetrized plot, the truncation of the data in t_2 trading off resolution for signal intensity. T_5 may be unambiguously assigned as the resonance at $\delta = -112.3$ ppm as it decreases significantly in intensity relative to the other signals if long enough delay times are not used, indicating that it has a much longer T_1 value. A major contribution to the relaxation mechanism is ^{29}Si dipolar interactions with molecular oxygen and T_5 is the only site which is not on the surface of a channel wall. From this assignment of T_5 one can proceed to assign the connectivities yielding the labeling of the cross-peaks given in Figure 21.

When the number of points in T_2 is increased to 450, the 2D plot shows the same connectivities but with a lower S/N as shown in Figure 22. Most importantly, doublet splittings are observed for the cross-peaks in F_2 (the limited resolution in F_1 precludes their observation in this dimension). Figure 22B shows plots of rows from this 2D experiment corresponding to the maxima in the diagonal peaks where the doublet structures are clearly observable. The observed splittings are all between 9 and 16 Hz, but these are approximate values only. These data may be compared

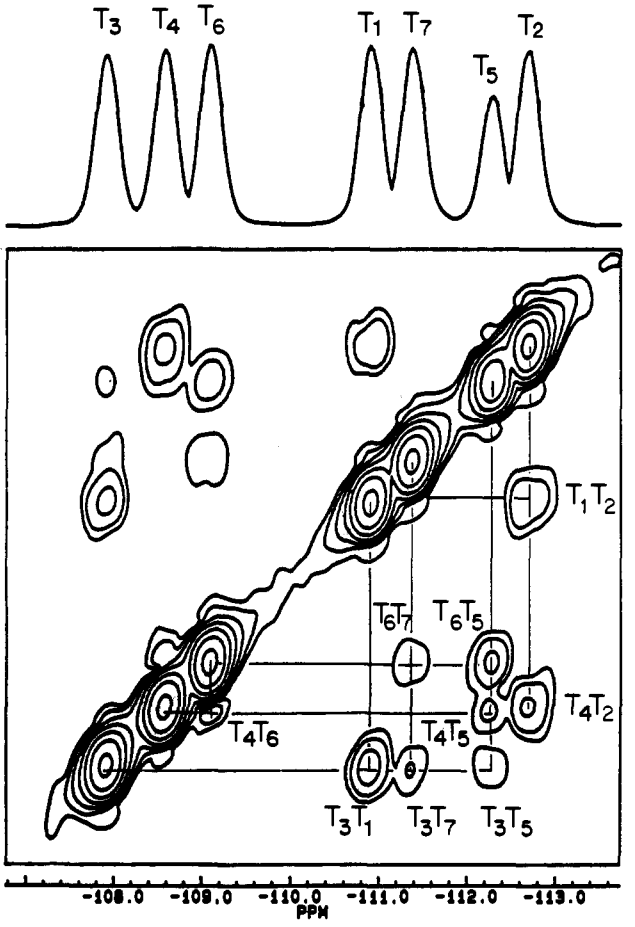

Figure 21. Contour plot of a COSY experiment on ZSM-12 with the projection in the F_2 dimension shown on top. The temperature was 300 K and 64 experiments were carried out with 160 scans in each experiment. A sweep width of 1200 Hz, a fixed delay of 5 ms, and 256 real data points were used for the data processing (reprinted from ref 44; copyright 1990 American Chemical Society).

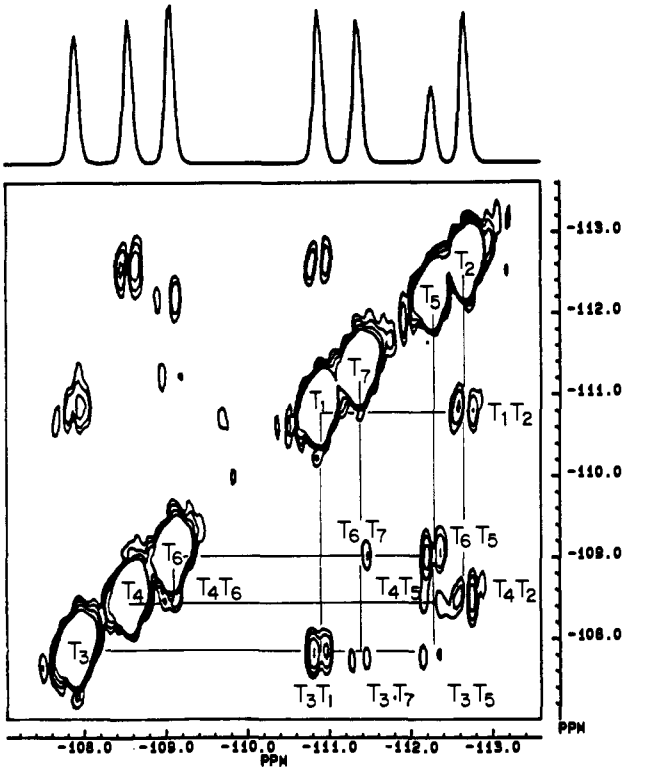

Figure 22. Contour plot of a COSY experiment on ZSM-12 with projection in F_2. The same conditions as those in Figure 21 were used except that 80 scans were taken in each experiment. Four hundred and fifty real data points and power calculation were used in the data analysis (reprinted from ref 44; copyright 1990 American Chemical Society).

with the ^{29}Si–O–^{29}Si couplings observed in alkaline silicate solutions enriched in ^{29}Si.[47] Silicon atoms in 4- and 5-membered rings in these species show couplings of the order of 10 Hz, approximately those observed in the present work and it is thus felt that the present data represent the first direct observation of scalar ^{29}Si–O–^{29}Si couplings in the solid state.

The observation of the scalar couplings is important in that it facilitates the application of the 2D INADEQUATE sequence. The result of such an experiment carried out with a conventional [(90°$_x$)–τ–(180°)–τ–(90°)–t_1–(135°)–t_2, acquire] sequence[49] where the value of τ is chosen to maximize the connectivities for a particular J coupling value. Compared to the COSY experiment, the INADEQUATE experiment has a number of advantages and disadvantages: In general, better S/N may be anticipated as there is a 2-fold decrease in the multiplicities of the cross-peaks, the main (noncoupled) center signals are subtracted, giving better dynamic range for the connectivities, and since the final signal is more constant in time, a much more efficient filter function can be used. In addition, any spinning rate may now be used, as spinning sidebands will not appear after analysis of the data. Furthermore, it is much easier to observe connectivities between resonances close in frequency which occur close to the large diagonal signals in the COSY experiment. The main potential disadvantage of the technique is that one must have a reasonable estimate of the scalar J coupling to choose the appropriate value of τ. If this can be done, all of the individual frequency-encoding experiments make an efficient contribution to the experiment (Figure 23), resulting in good S/N as noted above. All of the connectivities found and assigned in the previous COSY experiments are confirmed in the INADEQUATE experiment, including that between T_4 and T_6, which is clearly resolved here but was ambiguous in the COSY experiment due to the close proximity of the cross-peaks to the diagonal. It should be noted that all of the assignments previously discussed could have been made from the INADEQUATE experiment without having to know the identity of T_5, the observation of the T_4T_6 connection giving increased confidence in the assignment as every single connectivity is now observed. As previously, the intensities of the signals qualitatively reflect the numbers of connections involved. The doublet structures are clearly observable in this experiment, again confirming the previous results. The resolved splittings from single rows in the 2D plot are in good agreement with the values previously found and do not change when the spinning rate is varied between 1.0 and 3.0 kHz. As in the previous example with the COSY experiment, only the rows show doublet structure due to the very limited resolution in F_1.

Similar agreement between the observed connectivities and those predicted from the structure are found in corresponding experiments on zeolite ZSM-22 giving further confidence in the reliability of these techniques and the demonstrated ability to perform them successfully on natural abundance materials greatly ex-

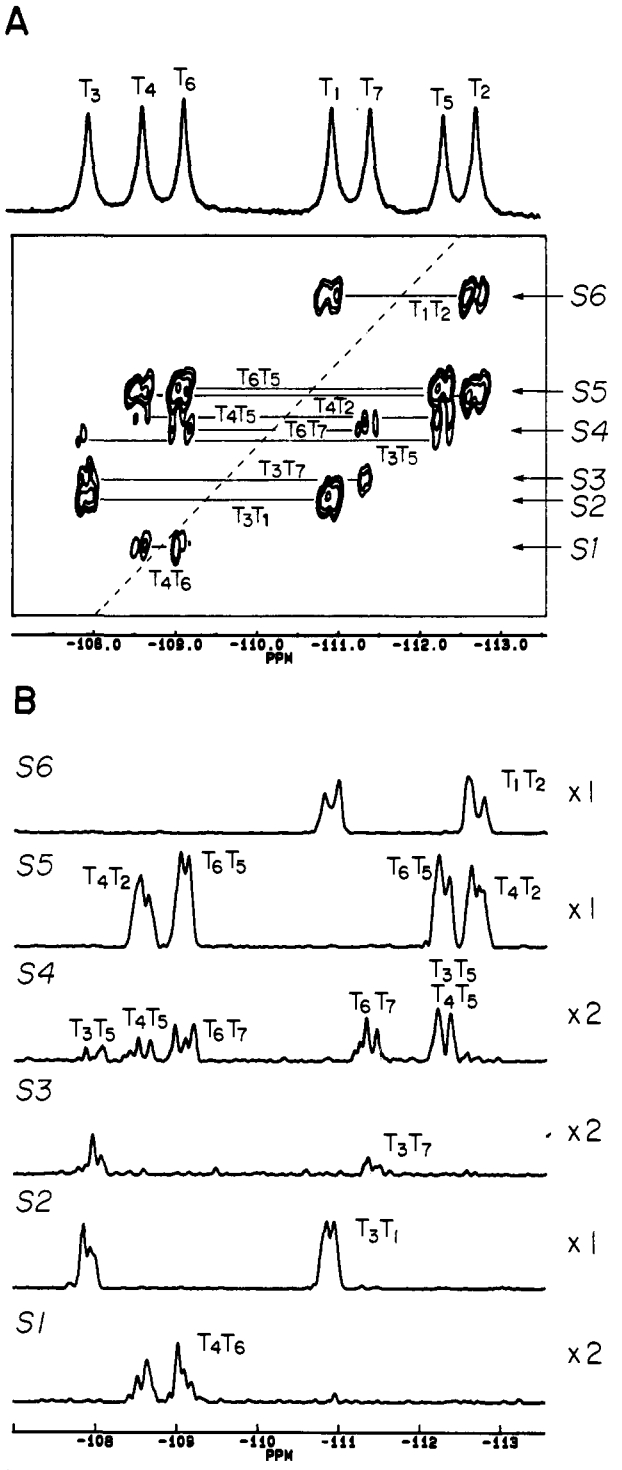

Figure 23. (A) Contour plot of an INADEQUATE experiment on ZSM-12 at 300 K with the 1D MAS NMR spectrum above with 52 experiments carried out, 64 scans per experiment, 800-Hz sweep width, fixed delay of 20 ms, and 450 data points collected during the acquisition. Since bell apodization and power calculations were used in the data processing. (B) Row plots from part A. The numbers of the rows correspond to those indicated in part A.

tends their potential. In both cases, the 2D INADEQUATE sequence gives superior performance, and this will usually be the experiment of choice.

Zeolite ZSM-5 has the most complex unit cell of any zeolite system and this represents a very demanding test of the reliability of these techniques, there being either 12 or 24 T sites in the structure depending on the phase. The different phases which have been investigated are summarized in Table II together with sources of the

TABLE II. Description of the Samples of ZSM-5 Investigated by ^{29}Si 2D NMR (adapted from ref 54; copyright 1990)

Sample	Sample and conditions	Space group (ref.)	T-sites in asymmetric unit	Name given in discussion
ZSM-5	Ambient temperature (300 K)	Monoclinic form P2/n (50)	24	Monoclinic phase
	High temperature (430 K)	Orthorhombic form Pnma (51)	12	Orthorhombic phase (12 T-sites)
ZSM-5 with sorbed *p*-xylene	Low-loading with *p*-xylene (2 molecules/UC, 300K)	Pnma (52)		
	High-loaded (8 molecules/UC, 293K)	Orthorhombic form $P2_12_12_1$ (53)	24	Orthorhombic phase (24 T-sites)

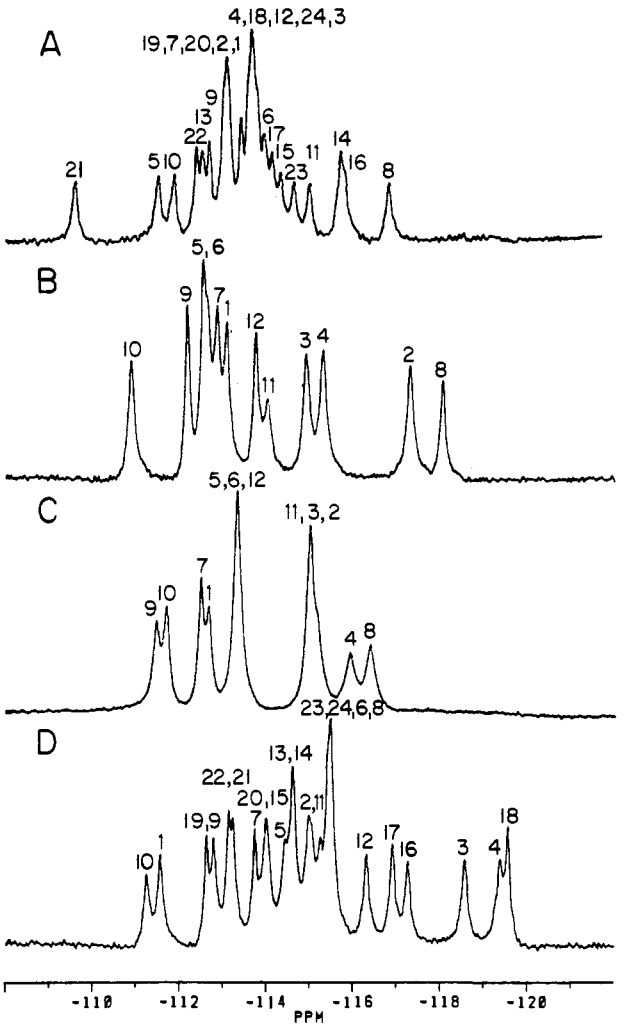

Figure 24. (A) ^{29}Si MAS NMR spectrum of ZSM-5 at 300 K. (B) ^{29}Si MAS NMR spectrum of low-loaded ZSM-5 (2 molecules) of *p*-xylene per 96 T atom unit cell) at 300 K. (C) ^{29}Si MAS NMR spectrum of ZSM-5 at 403 K. (D) ^{29}Si CP/MAS NMR spectrum of high-loaded ZSM-5 (8 molecules of *p*-xylene per 96 T atom unit cell) at 293 K. The assignments of the individual resonances of the four spectra are indicated (reprinted from ref 54; copyright 1990 American Chemical Society).

structural data. It should be noted that good single-crystal refinements have recently become available from the work of van Koningsveld and co-workers on the room-temperature, high-temperature, and high-loaded (8 molecules per unit cell of *p*-xylene) forms which can

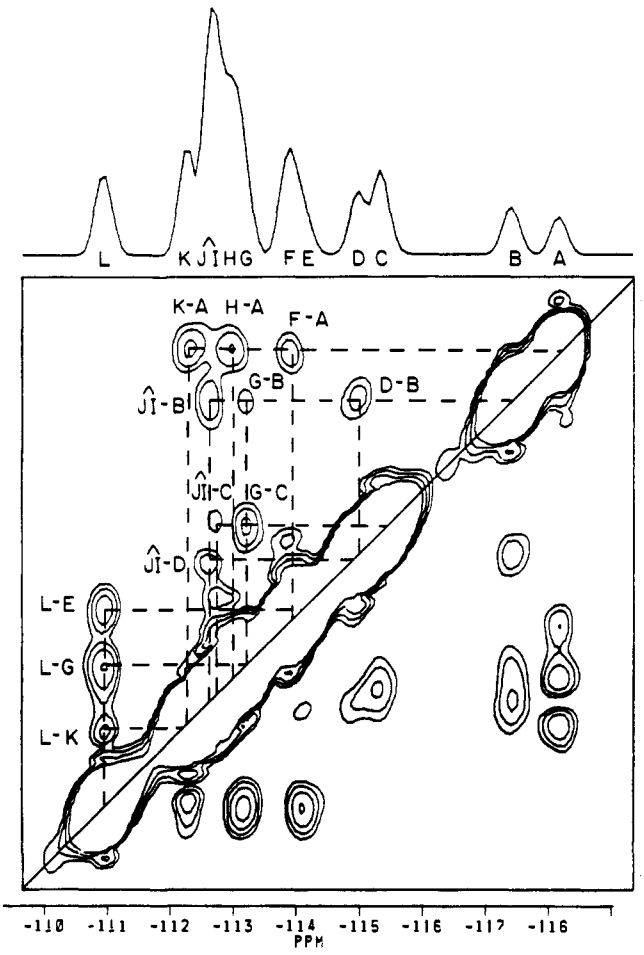

Figure 25. Contour plot of a COSY-45 experiment on ZSM-5 with 2 molecules of *p*-xylene per unit cell with the projection in the F_2 dimension shown above. The temperature was 300 K, and 64 experiments were carried out with 576 scans in each experiment. A sweep width of 1700 Hz, a fixed delay of 10 ms, and 220 real data points were used. Sine-bell-squared apodization and power calculation were used for the data processing (reprinted from ref 54a; copyright 1990 American Chemical Society).

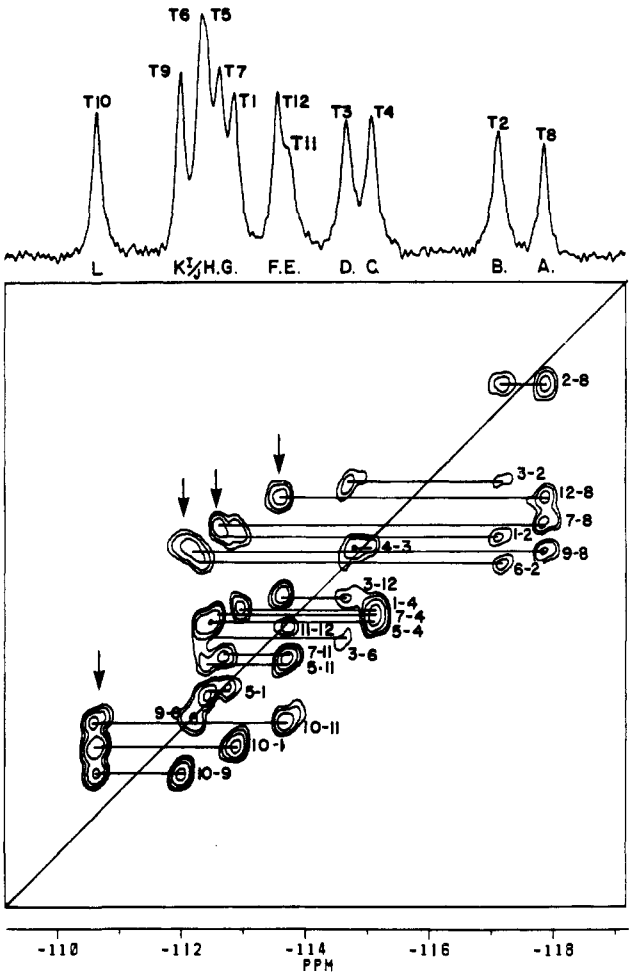

Figure 26. Contour plot of an INADEQUATE experiment on ZSM-5 with 2 molecules of *p*-xylene per unit cell carried out at 300 K with a 1D MAS NMR spectrum shown above. Thirty-six experiments with 512 scans in each experiment were performed with a recycle time of 14 s, and the total time for the experiment was approximately 72 h. A sweep width of 800 Hz, a fixed delay of 15 ms, and 140 real data points were used. Sine-bell and trapezoidal apodizations in the F_2 and F_1 dimensions, respectively, and a power calculation were used for data processing (reprinted from ref 54; copyright 1990 American Chemical Society).

be used together with the NMR data.[50,51,53]

Figure 24 shows the 1D NMR spectra of the four phases together with the detailed assignments of the resonances in terms of the corresponding unit cells shown in the figure.[54] It is outside the scope of the present review to describe in detail the results and the reasoning behind these assignments but typical data from the orthorhombic form with two molecules of *p*-xylene are presented in Figures 25 and 26. There are 22 ^{29}Si–O–^{29}Si connectivities expected in total for this phase and a total of 12 are observed in the COSY experiment. The main problem is the large spectral density in the centre of the 1D spectrum which means that many of the cross-peaks in the 2D spectrum will occur close to the diagonal. The corresponding INADEQUATE spectrum (Figure 26) is superior with 21 of the 22 connectivities being clearly observed. From the knowledge that only four silicons have self-connectivities and using general structural information from the X-ray data on all the phases, a complete self-consistent assignment can be made as indicated in the figure.[54]

The reliability of these 2D connectivity experiments is now well enough established that they can be used with confidence in the investigation of unknown structures in conjunction with diffraction studies. In a first step in this direction, a study of the three-dimensional bonding connectivities in ZSM-11 in both its high- and low-temperature forms has been reported.[55] As described earlier these are related to each other by a temperature-induced phase transition. The high-temperature form is known to have tetragonal symmetry with space group $I\bar{4}m2$, while the details of the ZSM-11 structure at low temperatures are not known to date from diffraction measurements.

2D INADEQUATE experiments at high temperature (340 K) confirmed the postulated structure. All of the nine expected connectivities were observed, as shown in Figure 27, permitting an unambiguous assignment of the spectrum. In the low-temperature (303 K) 2D experiments, enough information was obtained, that combined with the knowledge of the high-temperature structure, a structure could be suggested for the low-temperature form. The complete connectivity pattern of the 12 T sites in the structure was established and at least one space group, $I\bar{4}$, is compatible with the NMR data. It is thus suggested that this is a possible space group for use in further diffraction investigations.[55]

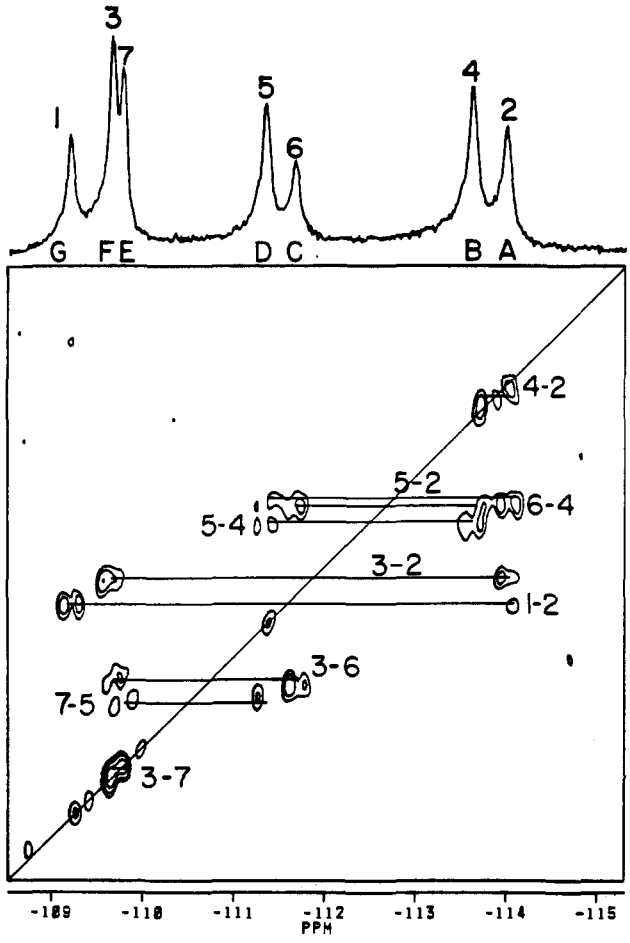

Figure 27. 2D INADEQUATE spectrum of ZSM-11 at 340 K (reprinted from ref 55; copyright 1991 American Chemical Society).

V. Studies of Other Nuclei in the Zeolite Framework (^{27}Al, ^{27}O, ^{1}H)

The other most abundant nuclei in the zeolite framework, ^{27}Al and ^{17}O, show a more complex behavior than ^{29}Si as they are quadrupolar nuclei with nonintegral spins (both with $I = {}^5/_2$). The effect of the quadrupolar interaction on the Zeeman splitting in such systems is illustrated in Figure 12 for a spin $^5/_2$ nucleus such as ^{27}Al. As can be seen (Figure 28), the $+{}^1/_2 \leftrightarrow -{}^1/_2$ transition is unaffected by the quadrupolar interaction to first order (both levels are shifted by the same amount in the same direction), and it is this transition that is observed. The other allowed transitions are usually too broad and shifted too far from resonance to be observed directly. The line shape due to the $+{}^1/_2 \leftrightarrow -{}^1/_2$ transition is distorted and shifted due to the second-order quadrupolar interaction. The shift in the center of gravity of this signal is given by

$$\omega_{CG} - \omega_0 = {}^1/_{30}(\omega_Q{}^2/\omega_0)\,[I(I+1) - {}^3/_4]\,(1 + {}^1/_3\eta^2) \quad (5)$$

where $\omega_Q = (3e^2qQ)/[2I(2I-1)h]$, eq is the z component of the electric field gradient tensor, eQ is the quadrupole moment of the nucleus, η is the asymmetry parameter, and ω_0 is directly proportional to the applied field. Therefore undesired shifts and line-shape distortions can be minimized by working at high fields. This is illustrated in Figure 29, which shows the ^{27}Al MAS NMR spectra of a zeolite-Y sample at 23.5 and 104.2 MHz. The high-field spectrum is much less distorted,

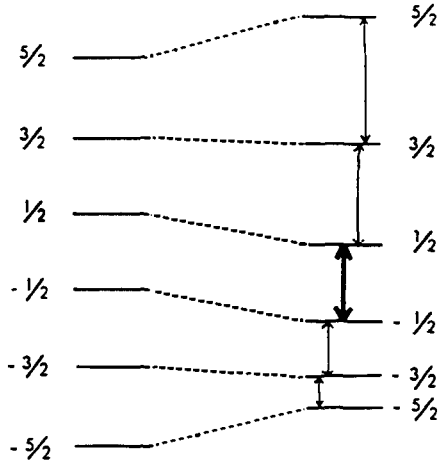

Figure 28. Energy level diagram for a spin $^5/_2$ nucleus showing the effect of the first-order quadrupolar interaction on the Zeeman energy levels. The ($m = {}^1/_2 = m = -{}^1/_2$) transition (shown in bold) is independent of the quadrupolar interaction to first order.

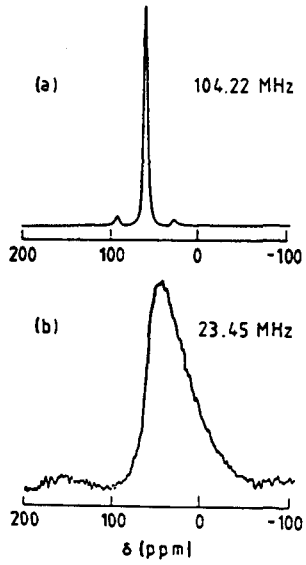

Figure 29. ^{27}Al MAS NMR spectra of zeolite-Y obtained at 23.45 and 104.22 MHz (proton frequencies 90 and 400 MHz, respectively) (from ref 6).

and the apparent chemical shift is much closer to the correct isotropic shift value. In the case of quadrupolar nuclei, the nuclear spin is not quantized along the Zeeman field direction, and MAS greatly reduces, but does not completely eliminate, the interaction. If the second-order quadrupolar interaction completely dominates the spectrum (as for example the case of ^{51}V in VO_3^- and V_2O_5[56]), spinning at an angle other than 54° 44′ may be employed to best reduce quadrupolar interaction, but other interactions such as the shift anistropy may increase, and an experimental compromise must often be sought. In any event, use of the highest possible field will be advantageous, and these experiments for the most part may be carried out again by using a conventional high-resolution spectrometer. ^{27}Al spectra of zeolites have been obtained at frequencies up to 154.5 MHz (600 MHz for protons).[57]

^{27}Al MAS NMR spectra of the tetrahaedral lattice aluminum in zeolites show only a single resonance because every Al has the environment Al[4Si], although the Al chemical shifts of individual zeolites have characteristic values. This is because Loewenstein's rule

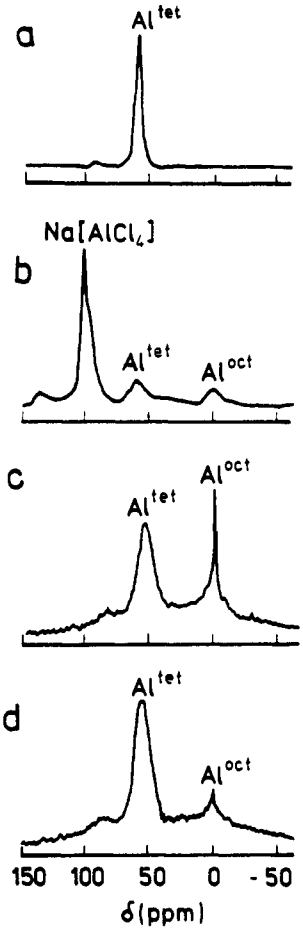

Figure 30. ^{27}Al MAS NMR spectra at 104.2 MHz obtained on zeolite-Y samples at various stages of the $SiCl_4$ dealumination procedure; (A) starting Faujasite sample, (B) intact sample after reaction with $SiCl_4$ before washing, (C) sample as in B after washing with distilled water, (D) after several washings (9) (adapted from ref 59; copyright 1983 American Chemical Society).

forbids Al–O–Al linkages and the primary information afforded by the ^{27}Al spectra is the coordination, discriminating between (i) octahedral coordination which gives a peak at about 0 ppm (with reference to $[Al(H_2O)_6]^{3+}\cdot H_2O$) and (ii) tetrahedral (lattice) coordination which occurs in the range of 50–65 ppm. It is not necessary to ^1H decouple in these experiments as the protons present are generally mobile and do not contribute greatly to the final ^{27}Al line widths. In order to obtain quantitative information, small Al pulse angles ($\leq 15°$) should be used.[58]

The sensitivity of the ^{27}Al spectra to coordination makes them ideal probes of reactions involving the zeolite lattices. As indicated previously, dealumination of the lattice can be achieved for some zeolites by treatment with silicon–tetrachloride ($SiCl_4$). The overall reaction which is postulated to occur is shown in eq 6. The ^{27}Al spectra (Figure 30) confirm the basic

$$SiCl_4 + Na_y(SiO_2)_x(AlO_2)_y \rightarrow Na_{(y-1)}(SiO_2)_{(x+1)}(AlO_2)_{y-1} + NaCl + AlCl_3 \quad (6)$$

$$NaCl + AlCl_3 \rightarrow Na^+AlCl_4^- \quad (7)$$

mechanism of eq 6 but reveal it to be more complex.[59] The top spectrum (Figure 30B), taken after reaction with $SiCl_4$ but before washing, shows that the tetrahedral (lattice) aluminum has greatly decreased, but there

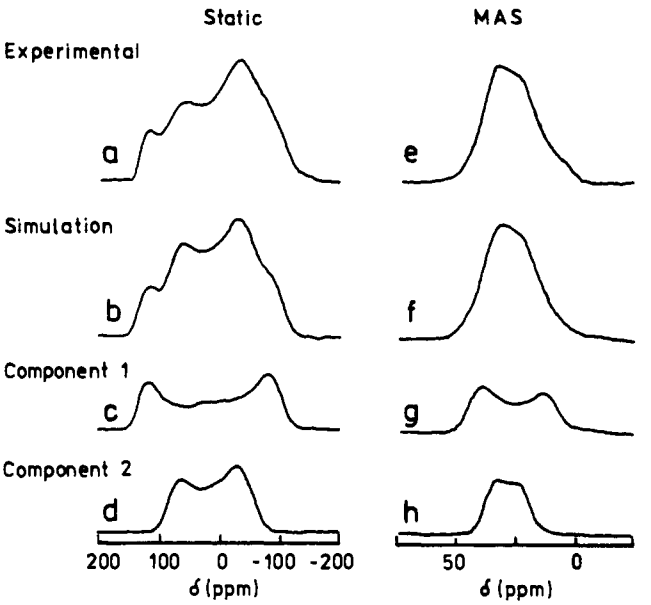

Figure 31. ^{17}O NMR spectra (67.8 MHz) and spectral simulations for NaY zeolite of Si/Al = 2.74: (a) static spectrum; (b) simulation of a using parameters of c and d; (c) component 1, Si–^{17}O–Si; (d) component 2, Si–^{17}O–Al; (e) MAS spectrum; (f) simulation of e, using parameters of g and h; (g) component 1,Si–^{17}O–Si; (h) component 2, Si–^{17}O–Al (reprinted from ref 63; copyright 1986 American Chemical Society).

is the appearance of a very intense absorption at about +100 ppm, which can be identified as being due to $AlCl_4^-$ from the high-temperature reaction of NaCl and $AlCl_3$ as indicated in eq 7. This peak is removed by subsequent washing, but much of the aluminum remains trapped in the cavities as octahedral aluminum species. Careful further washing and if necessary, ion exchange is needed to remove more completely nonlattice aluminum (bottom spectrum, Figure 30D). The broad resonances under the spectra (C,D) indicate the presence of aluminum atoms in asymmetric environments. The presence of aluminum nuclei in distorted environments is a difficult problem as the quadrupolar broadening could become severe enough to preclude observation of a signal. A number of authors have proposed treatment with acac to convert extra-lattice aluminum species to $Al(acac)_3$ which can easily be observed due to its highly symmetric octahedral environment.[60] In other work, ^{27}Al nutation NMR experiments have been used[61,62] but neither of these approaches have yielded a completely satisfactory detailed description of the range of aluminum environments in chemically modified zeolites.

Particularly important from the point of view of the lattice structures are ^{17}O spectra which will be affected by both chemical shift affects and the second-order quadrupolar interaction. As shown by Oldfield and co-workers,[63] by investigation of selected reference samples, the important contributing factors can be delineated. The ^{17}O spectrum of zeolite-A which has only Si–^{17}O–Al environments shows a relatively small quadrupolar coupling while highly siliceous zeolite-Y which contains only Si–^{17}O–Si environments exhibits a pronounced quadrupolar interaction. Thus, the ^{17}O spectra of low Si/Al ratio zeolites may be deconvoluted in terms of the contributions of these two components (1 and 2 corresponding to Si–O–Si and Si–O–Al) as shown in Figure 31 for zeolite-Y with Si/Al = 2.74. It

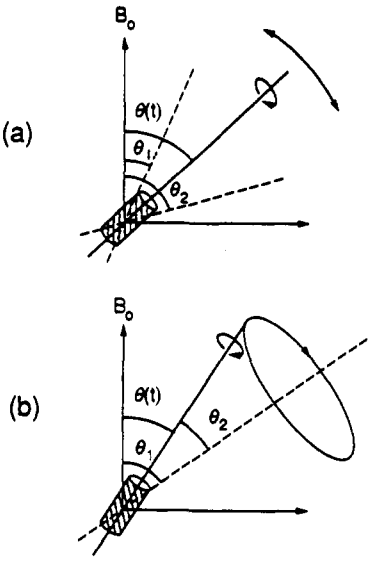

Figure 32. Schematic representation of the two approaches for averaging second-order interactions: (a) dynamic angle spinning and (b) double rotation (from ref 68).

should be noted that it is the static spectra which are most informative here since the (larger) quadrupolar effect is dominant. That is, "resolution" is the relative separation of spectroscopic features, not simply the width of the resonances. The Si/Al ratios can be calculated from the relative Si–^{17}O–Al and Si–^{17}O–Si concentrations in a manner analogous to that described earlier. Again, the ratio is that for the framework elements only.

A most promising recent development which is relevant to both ^{27}Al and ^{17}O investigations has been the introduction of experiments in which the spinner axis undergoes a time-dependent trajectory with respect to the magnetic field axis, designed to average second-order as well as first-order interactions. In double rotation experiments (DOR), the axis of the rotor is moved continuously in a cone by spinning the sample in a spinner within another spinner as shown in Figure 32a. By the correct choice of angles for the two spinner axes, second-order effects are averaged. In the case of dynamic-angle spinning (DAS), the sample is contained within a single spinner but the orientation axis of the spinner is switched between two discrete angles with respect to the external magnetic field (Figure 32b). A whole set of complementary angles are available, but different times must be spent by the sample at each of the orientations depending on the particular pair of angles chosen. For the complementary angles θ_1 = 37.38°, θ_2 = 79.19°, equal times are spent at both angles.[67,68]

The power of this approach in the removal of second-order quadrupolar interactions compared to previous experiments is well illustrated in Figure 33. The ^{17}O DAS spectrum clearly shows the single oxygen site expected for this system.[68] More recently, DOR and DAS ^{17}O spectra have been reported for a variety of silicates.[69] In all cases, narrow lines were observed, which could be related to the number of crystallographically inequivalent sites in much the same way as was possible for the ^{29}Si MAS spectra discussed earlier. Although ^{17}O results on zeolites have not been reported to date, these will no doubt be forthcoming. Similarly, although there are no ^{27}Al data on these systems, con-

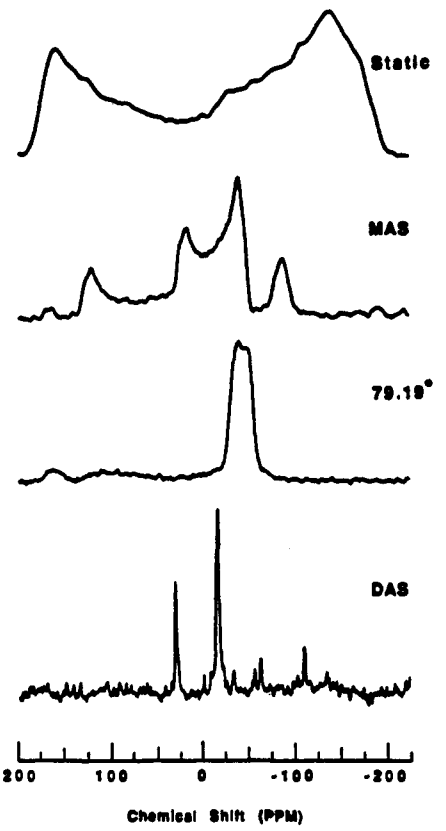

Figure 33. The oxygen-17 static, MAS, variable-angle spinning (at 79.19°), and one-dimensional DAS spectra for cristobalite. The single oxygen isotropic shift is at −16.6 ppm with respect to $H_2{}^{17}O$ (from ref 68).

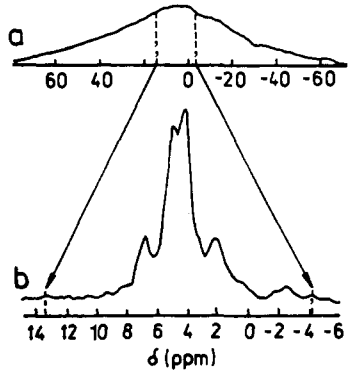

Figure 34. Line narrowing by the MAS technique of the 270 MHz ^{1}H NMR spectrum of a dehydrated HY zeolite: (a) static powder spectrum; (b) MAS spectrum at 2.5-kHz rotation frequency (sealed glass ampoule) (from ref 71c).

siderable line narrowing was observed in the closely related ALPO system VPI-5 in ^{27}Al spectra obtained as a function of hydration.[70]

One last experiment important in a consideration of framework nuclei which is particularly informative, involves the detection and characterization of the proton sites within the zeolite structure as pioneered by Freude and Pfeifer.[71] Even when the protons are not major contributors to the overall lattice structure, they may be central to the catalytic reactions. Since they are relatively dilute in the lattice, a simple MAS experiment yields spectra of sufficient resolution to identify the different functionalities as shown in Figure 34. Spectra of this type will be critical in the probing of the catalytic activities of these systems and the op-

timization of techniques for their activation.

Acknowledgments. The authors acknowledge the financial assistance of NSERC Canada in the form of Operating and Major Equipment Grants (C.A.F.). G.T.K. acknowledges the assistance of the Alexander von Humboldt Foundation in the form of a Senior Scientist Award. Y.F. thanks the University of British Columbia for the award of a University Graduate Fellowship.

References

(1) Engelhardt, G.; Michel, D. *High-Resolution Solid-State NMR of Zeolites and Related Systems*; John Wiley and Sons: London, 1987.
(2) (a) Meier, W. M. In Molecular Seives. *SCI Mong.* **1968**. (b) Breck, D. W. *Zeolite Molecular Sieves*; Wiley Interscience: New York, 1974.
(3) (a) Smith, J. V. *Zeolite Chemistry and Catalysis*; Rabo, J. A., Ed. ACS Monograph Series 171, American Chemical Society: Washington, DC, 1976. (b) Barrer, R. M. *Zeolites and Clay Minerals as Sorbents and Molecular Sieves*; Academic Press: London, 1978.
(4) (a) U.S. Patent 3, 702, 886, 1972. (b) Kokotailo, G. T.; Lawton, S. L.; Olson, D. H.; Meier, W. *Nature* **1978**, *272*, 437. (c) Kokotailo, G. T.; Meier, W. M. *SCI Monogr.* **1980**, *10*.
(5) (a) Meier, W. M.; Olson, D. H. *Atlas of Zeolite Structure Types*; Structure Commission of the International Zeolite Association, Butterworths: London, 1978. (b) It has recently been demonstrated that the use of synchrotron X-ray sources permits single-crystal studies to be carried out on much smaller samples. Eisenberger, P.; Newsam, J. B.; Leonowicz, M. E.; Vaughan, D. E. W. *Nature* **1984**, *309*, 45. (c) The use of Rietveld refinement techniques allows better structural information to be obtained from powder diffraction data. David, W. I. F.; Harrison, W. T. A.; Johnson, M. W. High Resolution Powder Diffraction. *Materials Science Forum*; Catlow, C. R. A., Ed.; Trans. Tech. Publication: Andermannsdorf, Switzerland, 1986; Vol. 9, pp 89–101.
(6) Fyfe, C. A.; Cobbi, G. C.; Hartman, J. S.; Lenkinski, R. E.; O'Brien, J. H.; Beange, E. R.; Smith, M. A. R. *J. Magn. Res.* **1982**, *47*, 168.
(7) (a) Lippmaa, E.; Magi, M.; Samoson, A.; Grimmer, A. R.; Engelhardt, G. *J. Am. Chem. Soc.* **1980**, *102*, 4889. (b) Lippmaa, E.; Magi, M.; Samoson, A.; Tarmak, M.; Engelhardt, G. *J. Am. Chem. Soc.* **1981**, *103*, 4992.
(8) Fyfe, C. A.; Thomas, J. M.; Klinowski, J.; Gobbi, C. G. *Angew. Chem.* **1983**, *95*, 257; *Angew. Chem., Int. Ed. Engl.* **1983**, *22*, 259.
(9) Klinowski, J.; Ramdas, S.; Thomas, J. M.; Fyfe, C. A.; Hartmann, J. S. *J. Chem. Soc., Farad. Trans. 2* **1983**, *78*, 1025.
(10) Loewenstein, W. *Am. Mineral.* **1954**, *39*, 92.
(11) Melchior, M. T. *A.C.S. Symp. Ser.* **1983**, *218*, 243.
(12) Engelhardt, G.; Lohse, U.; Samoson, A.; Magi, M.; Tarmak, M.; Lippmaa, E. *Zeolites* **1982**, *2*, 59.
(13) (a) Fyfe, C. A.; Kokotailo, G. T.; Kennedy, G. J.; Gobbi, G. C.; DeSchutter, C. T.; Ozubko, R. S.; Murphy, W. J. *Proc. Int. Symp. Zeolite 85*, Elsevier, Ed.: Draj, B., Hocevar, D., Pjenovich, S., Eds.; Elsevier: Amsterdam, 1985; p 219. (b) Kokotailo, G. T.; Fyfe, C. A.; Kennedy, G. J.; Gobbi, G. C.; Strobl, H. J.; Pasztor, C. T.; Barlow, G. E.; Bradley, S.; Murphy, W. J.; Ozubko, R. S. *Pure Appl. Chem.* **1986**, *58*, 1367.
(14) Fyfe, C. A.; Kennedy, G. J.; Kokotailo, G. T.; DeSchutter, C. T. *J. Chem. Soc., Chem. Commun.* **1984**, 1093.
(15) Fyfe, C. A.; Gobbi, G. C.; Murphy, W. J.; Ozubko, R. S.; Slack, D. A. *Chem. Lett.* **1983**, 1547.
(16) Fyfe, C. A.; Gobbi, G. C.; Murphy, W. J.; Ozubko, R. S.; Slack, D. A. *J. Am. Chem. Soc.* **1984**, *106*, 4435.
(17) Fyfe, C. A.; Gobbi, G. C.; Kennedy, G. J.; Graham, J. D.; Ozubko, R. Z.; Murphy, W. J.; Bothner-By, A.; Dadok, J.; Chesnick, A. S. *Zeolites* **1985**, *5*, 179.
(18) Fyfe, C. A.; Kokotailo, G. T.; Kennedy, G. J.; DeSchutter, C. T. *J. Chem. Soc., Chem. Commun.* **1985**, 306.
(19) Fyfe, C. A.; Gobbi, G. C.; Klinowski, J.; Thomas, J. M.; Ramdas, S. *Nature* **1982**, *296*, 530.
(20) Fyfe, C. A.; Kennedy, G. J.; DeSchutter, C. T.; Kokotailo, G. T. *J. Chem. Soc., Chem. Commun.* **1984**, 541.
(21) West, G. W. *Aust. J. Chem.* **1984**, *37*, 455.
(22) Fyfe, C. A.; Kennedy, G. J.; Kokotailo, G. T.; Lyerla, J. R.; Fleming, W. W. *J. Chem. Soc., Chem. Commun.* **1985**, 740.
(23) Hay, D. G.; Jaeger, H.; West, G. W. *J. Phys. Chem.* **1985**, *89*, 1070.
(24) Fyfe, C. A.; O'Brien, J. H.; Strobl, H. *Nature* **1987**, *363*, 6110.
(25) Fyfe, C. A.; Strobl, H.; Kokotailo, G. T.; Kennedy, G. J.; Barlow, G. E. *J. Am. Chem. Soc.* **1988**, *110*, 3373.
(26) (a) U.S. Patent 3,709,979, 1973. (b) Kokotailo, G. T.; Chu, P.; Lawton, S. L.; Meier, W. M. *Nature* **1978**, *275*, 119.
(27) (a) Fyfe, C. A.; Kokotailo, G. T.; Kennedy, G. J.; DeSchutter, C. T. *J. Chem. Soc., Chem. Commun.* **1985**, *306*. (b) Fyfe, C. A.; Gies, H.; Kokotailo, G. T.; Pasztor, C.; Strobl, H.; Cox, D. E. *J. Am. Chem. Soc.* **1989**, *111*, 2470.
(28) U.S. Patent 4,287,166, 1981.
(29) Schlenker, J. L.; Dwyer, F. G.; Jenkins, E. E.; Rohrbaugh, W. J.; Kokotailo, G. T.; Meier, W. M. *Nature* **1981**, *294*, 340.
(30) (a) Gies, H.; Liebau, F.; Gerke, H. *Angew. Chem.* **1982**, *94*, 214. (b) Gies, H. *Z. Kristallogr.* **1984**, *167*, 73.
(31) Strobl, H.; Fyfe, C. A.; Kokotailo, G. T.; Pasztor, C. T. *J. Am. Chem. Soc.* **1987**, *109*, 4733.
(32) (a) Benn, R.; Günther, H. Modern Pulse Methods in High Resolution NMR Spectroscopy. *Angew. Chem., Int. Ed. Engl.* **1983**, *22*, 250. (b) Bax, A. *Two Dimensional Nuclear Magnetic Resonance in Liquids*; Delft University Press: Delft, The Netherlands, 1982. (c) Derome, A. E. *Modern NMR Techniques for Chemistry Research*; Pergamon Press: Oxford, England, 1987. (d) Sanders, J.; Hunter, B. *Modern NMR Spectroscopy, A Guide for Chemists*; Oxford University Press: Oxford, England, 1987.
(33) Szeverenyi, N. M.; Sullivan, M. J.; Maciel, G. E. *J. Magn. Reson.* **1982**, *47*, 462.
(34) Bax, A.; Szeverenyi, N. M.; Maciel, G. E. *J. Magn. Reson.* **1983**, *51*, 400.
(35) (a) Opella, S. J.; Waugh, J. S. *J. Chem. Phys.* **1977**, *66*, 4919. (b) Bodenhausen, G.; Stark, R. E.; Ruben, D. J.; Griffin, R. G. *Chem. Phys. Lett.* **1979**, *67*, 424.
(36) Caravatti, P.; Deli, J. A.; Bodenhausen, G.; Ernst, R. R. *J. Am. Chem. Soc.* **1982**, *104*, 5506.
(37) Frey, M. H.; Opella, S. J. *J. Am. Chem. Soc.* **1984**, *106*, 4942.
(38) Benn, R.; Grondey, H.; Brevard, C.; Pagelot, A. *J. Chem. Soc., Chem. Commun.* **1988**, 102.
(39) Fyfe, C. A.; Gies, H.; Feng, Y. *J. Chem. Soc., Chem. Commun.* **1989**, 1240.
(40) Fyfe, C. A.; Gies, H.; Feng, Y. *J. Am. Chem. Soc.* **1989**, *111*, 7702.
(41) Fyfe, C. A.; Gies, H.; Feng, Y.; Grondey, H. *Zeolites* **1990**, *10*, 278.
(42) Gies, H. *Z. Kristallogr.* **1986**, *175*, 93.
(43) Fyfe, C. A.; Gies, H.; Feng, Y.; Kokotailo, G. T. *Nature* **1989**, *341*, 223.
(44) Fyfe, C. A.; Feng, Y.; Gies, H.; Grondey, H.; Kokotailo, G. T. *J. Am. Chem. Soc.* **1990**, *112*, 3264.
(45) LaPierre, R. B.; et al. *Zeolites* **1985**, *5*, 346.
(46) Fyfe, C. A.; Gies, H.; Kokotailo, G. T.; Marler, B.; Cox, D. E. Submitted for publication.
(47) Muller, L.; Kumar, A.; Ernst, R. R. *J. Chem. Phys.* **1975**, *63*, 5490.
(48) Harris, R. K.; Knight, C. T. G. *J. Chem. Soc., Faraday Trans. 2* **1983**, 1539.
(49) (a) Bax, A.; Freeman, R.; Frenkiel, T. A.; Levitt, M. H. *J. Magn. Reson.* **1981**, *43*, 478. (b) Mareci, T. H.; Freeman, R. *J. Magn. Reson.* **1982**, *48*, 158.
(50) van Koningsveld, H.; Jansen, J. C.; van Bekkum, H. *Zeolites* **1990**, *10*, 235.
(51) van Koningsveld, H.; et al. *Acta Cryst. B.*, in press.
(52) Gies, H.; Marler, B.; and co-workers. Unpublished work.
(53) van Koningsveld, H.; Tuinstra, F.; van Bekkum, H.; Jansen, J. C. *Acta Crystallogr.* **1989**, *B45*, 423.
(54) (a) Fyfe, C. A.; Grondey, H.; Feng, Y.; Kokotailo, G. T. *J. Am. Chem. Soc.* **1990**, *112*, 8812. (b) Fyfe, C. A.; Grondey, H.; Feng, Y.; Kokotailo, G. T. *Chem. Phys. Lett.* **1990**, *173*, 211. (c) Fyfe, C. A.; Feng, Y.; Grondey, H.; Kokotailo, G. T. *J. Chem. Soc., Chem. Commun.* **1990**, 1224.
(55) Fyfe, C. A.; Feng, Y.; Grondey, H.; Kokotailo, G. T.; Mar, A. *J. Phys. Chem.* **1991**, *55*, 3747.
(56) Meadows, M. D.; Smith, K. A.; Kisney, R. A.; Rothgels, T. M.; Skarjunl, R. P.; Oldfield, E. *Proc. Natl. Acad. Sci. U.S.A.* **1982**, *79*, 1351.
(57) Fyfe, C. A.; Gobbi, G. C.; Murphy, W. J.; Ozubko, R. S.; Slack, D. A. *J. Am. Chem. Soc.* **1984**, *106*, 4435.
(58) Samoson, A.; Lippmaa, E. *Phys. Rev. B* **1983**, *28*, 6567.
(59) Klinowski, J.; Thomas, J. M.; Fyfe, C. A.; Gobbi, G. C.; Hartman, J. S. *Inorg. Chem.* **1983**, *22*, 63.
(60) Grobet, P. J.; Geerts, H.; Tielen, M.; Martens, J. A.; Jacobs, P. A. In *Zeolites as Catalysts, Sorbents and Detergent Builders*; Elsevier: Amsterdam, 1989; p 721.
(61) Kentgers, A. P. M. Ph.D. Thesis, University of Nijmegen, Holland, 1987.
(62) Hamadan, X.; Klinowski, J. *A.C.S. Symp. Ser.* **1989**, *398*, 448; 465.
(63) Timken, H. K. C.; Turner, G. L.; Gilson, J. P.; Welsh, L. B.; Oldfield, E. *J. Am. Chem. Soc.* **1986**, *108*, 7231.
(64) Llor, A.; Virlet, J. *Chem. Phys. Lett.* **1988**, *152*, 248.
(65) Samoson, A.; Lippmaa, E.; Pines, A. *Mol. Phys.* **1988**, *65*, 1013.
(66) Chingas, G. C.; Lee, C. J.; Lippmaa, E.; Mueller, K. T.; Pines, A.; Samoson, A.; Sun, B. Q.; Suter, D.; Terao, T. In *Proceedings, XXIV Congress Ampere, Poznan, 1988*; Stankowski, J.,

Pislewski, N., Idziak, S., Eds.; D62, 1988.
(67) Chmelka, B. F.; Mueller, K. T.; Pines, A.; Stebbins, J.; Wu, Y.; Zwanziger, J. W. *Nature (London)* **1989**, *339*, 42.
(68) Mueller, K. T.; Sun, B. Q.; Chingas, G. C.; Zwanziger, J. W.; Terao, T.; Pines, A. *J. Magn. Res.* **1990**, *86*, 470.
(69) Mueller, K. T.; Wu, Y.; Chmelka, B. F.; Stebbins, J.; Pines, A. *J. Am. Chem. Soc.* **1991**, *113*, 32.
(70) Wu, Y.; Chmelka, B. F.; Pines, A.; Davis, M. E.; Grobet, P. J.; Jacobs, P. A. *Nature* **1990**, *346(6284)*, 550.
(71) (a) Freude, D.; Hunger, M.; Pfeifer, H. *Chem. Phys. Lett.* **1982**, *91*, 307. (b) Freude, D. *Adv. Colloid Interace Sci.* **1985**, *23*, 21. (c) Pfeifer, H.; Freude, D.; Hunger, M. *Zeolites* **1985**, *5*, 273. (d) Hunger, M.; Freude, D.; Pfeifer, H.; Schwieger, W. *Chem. Phys. Lett.* **1990**, *167*, 21.